Scientific Reports

https://doi.org/10.1038/s41598-026-54140-9

Article in Press

Productivity evaluation, multi-scale characterisation, and safety assessment of biochar derived from green and woody agricultural biomass in Qatar

Received: 27 February 2026

Accepted: 18 May 2026

Published online: 25 May 2026

Cite this article as: Al-Gaashani R., Shahid O., Wada O.Z. *et al.* Productivity evaluation, multi-scale characterisation, and safety assessment of biochar derived from green and woody agricultural biomass in Qatar. *Sci Rep* (2026). https://doi.org/10.1038/s41598-026-54140-9

Rashad Al-Gaashani, Omar Shahid, Ojima Z. Wada, Simjo Simson, Tricia A. Gomez, Mujaheed Pasha, Omar El Hassan, Abdulaziz Suwailem, Kashif Rasool, Gordon McKay, Tareq Al-Ansari & Khaled A. Mahmoud

Productivity Evaluation, Multi-Scale Characterisation, and Safety Assessment of Biochar Derived from Green and Woody Agricultural Biomass in Qatar

Rashad Al-Gaashani[a,*], Omar Shahid[b], Ojima Z. Wada[a], Simjo Simson[a], Tricia A. Gomez[a], Mujaheed Pasha[c], Omar El Hassan[c], Abdulaziz Suwailem[c], Kashif Rasool[a], Gordon McKay[b], Tareq Al-Ansari[a,b], Khaled A. Mahmoud[a]

[a]Qatar Environment and Energy Research Institute (QEERI), Hamad Bin Khalifa University (HBKU), Qatar Foundation, 34110 Doha, Qatar

[b]Division of Sustainable Development, College of Science and Engineering, Hamad Bin Khalifa University, Qatar Foundation, Doha, Qatar

[c]HBKU Core Labs, Hamad Bin Khalifa University, Qatar Foundation, Doha, Qatar

***Corresponding author.** Tel: 0097430571456. E-mail: ralgaashani@hbku.edu.qa*

Abstract:

Qatar produces approximately 2 million tons of agricultural biomass waste annually. Less than 20% is currently recycled or valorized, mainly through limited composting, landfilling, and, in some cases, open burning. This study presents a systematic production and multi-scale characterization of biochar derived from local mixed green agricultural waste (GAGW) and W, providing a characterization-based foundation to inform their potential integration into the energy-water-food (EWF) nexus of arid regions. Each feedstock was analyzed for moisture content (MC), volatile matter (VM), ash content, fixed carbon (FC), elemental composition (C, H, N, S), molar ratios (H/C, O/C), structural, elemental, morphological, thermal combustion and specific surface area properties. The experimental design follows a double-split arrangement. GAGW and WAGW were considered as the main plots, pyrolysis temperature (300, 400, 500, and 600 °C) as the sub-main plots, and residence time (20, 60, 90, and 120 min) as the sub-sub plots. Results demonstrate a fundamental divergence in carbonization pathways. WAGW

achieved a peak solid yield of 71.28% at 300 °C in 20 min, significantly outperforming GAGW (60%). As thermal severity increased to 600 °C, WAGW underwent superior structural development, reaching a specific surface area of 684 m^2/g, about 3 times higher than GAGW. Van Krevelen analysis validated the transition to highly recalcitrant aromatic frameworks, with WAGW reaching a superior H/C ratio of 0.30 compared to 0.35 for GAGW. While WAGW produced a carbon-dense matrix (82.6 atom% C), GAGW evolved into a nutrient-active medium, concentrating potassium (88,780 mg/kg) and calcium (63,932 mg/kg) in stable sylvite and calcite phases, as affirmed via X-ray Diffraction (XRD). Crucially, all produced biochar samples were free from hazardous heavy metals (As, Cd, Cr, Pb, Hg < 0.1 mg/kg), confirming their safety profile and suitability for further evaluation in potential soil and water applications.

Keywords: Biochar; Pyrolysis; Biomass; Agricultural Waste; Safety Assessment

Graphical Abstract

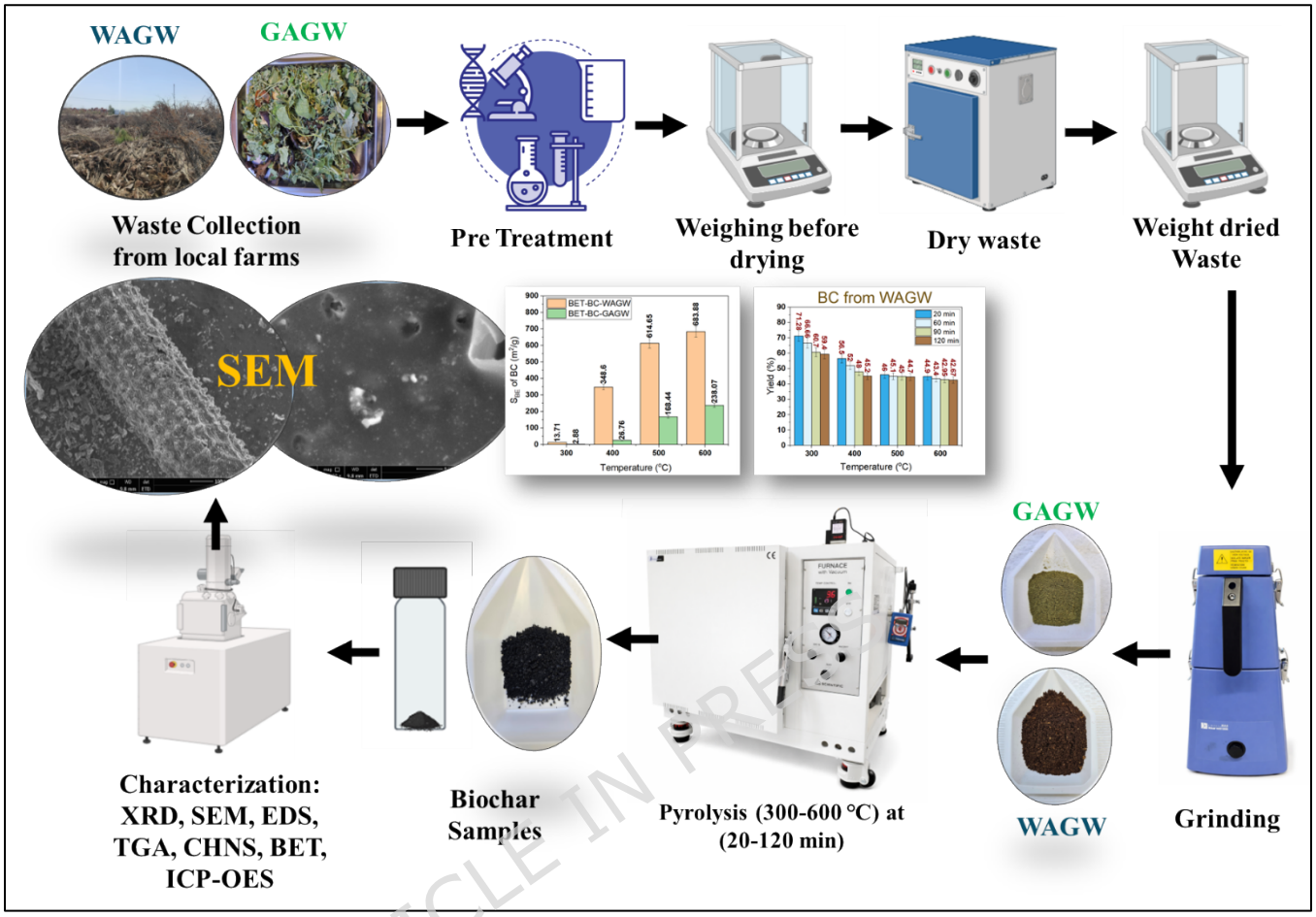

1. Introduction

The world's production of agricultural waste is estimated to be 1.3 to 2.1 billion tons [1-4]. In Qatar, more than 2 million tons of agricultural waste is produced annually, including waste from farms and livestock. Due to high living standards, the country is positioned as one of the top 3 countries globally for waste production per capita (1.8 kg per day) [5,6]. However, less than 20% of this waste is recycled or reused, indicating a significant opportunity to develop innovative ways to manage these resources more efficiently. Slow pyrolysis is an established thermochemical valorization process for biomass, yielding value products like biochar, tar, and syngas [7].

However, this method has not been extensively considered for the country's growing agricultural biomass waste. The current prevalent waste management practice via landfilling, along with incomplete combustion, represents a significant source of greenhouse gas emissions and other associated adverse environmental impacts [8,9]. Thus, there is a global push to explore sustainable alternatives, with increasing attention given to thermochemical conversion technologies, particularly pyrolysis, which enable biomass valorization into stable carbon form (biochar) [10,11].

Biochar is a stable, carbon-rich byproduct from biomass pyrolysis. It has long been recognized for its ability to sequester carbon in the soil, thus mitigating climate change. Biochar produced from different biomass materials has been studied worldwide for its potential to improve soil fertility, enhance water retention, facilitate pollutant adsorption in water, and for gas capture [12]. Several studies on biochar's efficacy in arid and semi-arid regions have affirmed their ability to improve soil quality and crop yield [13-16]. However, the properties and effectiveness of biochar are highly dependent on the feedstock used and the pyrolysis conditions. While previous local studies have closely examined other waste biomass sources like sludge and food waste [17-23]. There is still insufficient data to support the widespread adoption of biochar from Qatar's budding agricultural sector. Therefore, further research is necessary to validate biochar's potential role in the local EWF nexus water treatment, through the valorization of abundant local agricultural biomass.

The suitability of biochar for environmental applications is commonly evaluated based on internationally recognized quality standards and application-specific criteria. For agricultural use, guidelines such as those established by the European Biochar Certificate[24] and the International Biochar Initiative emphasize parameters including low concentrations of potentially toxic elements, appropriate pH, high organic carbon content, and stable aromatic structure to ensure soil safety and long-term carbon sequestration[25-27]. In addition, nitrogen content and nitrogen-containing functional groups play a key role in improving soil fertility and nutrient retention[28]. In contrast, biochar intended for water treatment applications is typically characterized by high specific surface area, well-developed porosity, and the presence of functional groups that enhance adsorption capacity for organic and inorganic contaminants. Several studies have demonstrated that biochar with BET surface areas exceeding 300 m^2/g and tailored surface chemistry exhibit high removal efficiencies for heavy metals and emerging pollutants. Therefore, aligning the physicochemical properties of produced biochar with these established criteria provides a rational basis for assessing its potential applicability in soil amendment and water treatment systems[24,29-31].

Pyrolysis temperature and residence time are key factors influencing biochar properties. Previous studies have shown that biochar is typically produced within a temperature range of 300–700 °C under oxygen-limited conditions, with temperature strongly influencing carbonization, aromaticity,

and surface development [32]. Lower temperatures (300–400 °C) favor higher yield and functional groups, while higher temperatures (500–700 °C) enhance carbonization and surface area [33,34]. Residence time also affects pore development, with moderate durations improving structural properties of biochar. BET and morphology are also significantly influenced by residence time (10-100 min) [35]. Therefore, the selected conditions (300–600 °C and 20–120 min) were chosen to systematically evaluate these effects, consistent with previous studies [32,36,37].

In this study, mixed green agricultural waste (GAGW) and woody agricultural waste (WAGW) were selected as representative feedstocks following consultation with local Qatari farms. This selection aims to address the environmental risks associated with improper disposal, such as pathogen transmission and greenhouse gas emissions from open burning. To provide a data-driven roadmap for their high-value valorization, the thermochemical evolution of these materials was systematically investigated. The study employed a rigorous experimental matrix with four pyrolysis temperatures (300-600 °C) and four residence times (20-120 min). The produced biochar samples were subjected to a multi-scale characterization suite. This included CHNS-O ultimate analysis, X-ray Diffraction (XRD), X-ray fluorescence (XRF), thermal gravimetric analysis (TGA), and field emission scanning electron microscopy (FE-SEM) combined with energy dispersive spectroscopy (EDS). These analyses were used to elucidate the complex trade-offs between solid yield, aromatization, and mineral concentration. Furthermore, a critical

safety assessment was conducted. Elemental screening for 31 target metals was performed using ICP-OES to establish a non-toxic baseline for environmental applications.

2. Materials and Methods

2.1. Feedstock collection and categorization

Feedstocks shown in Fig. 1 for biochar production were selected in consultation with two local farms in Qatar, based on availability and local agricultural practices. Eleven agricultural waste samples were collected and classified into GAGW and WAGW. GAGW included soft biomass such as leaves, stems, and dried vegetables, while WAGW comprised lignocellulosic materials such as date palm residues and Sidra branches. Prior to pyrolysis, all feedstocks were cleaned, dried to eliminate residual moisture, and ground to ensure uniformity for thermal conversion and characterization. This systematic categorization and preparation ensured a reliable basis for comparing the pyrolysis behavior and resulting biochar properties across a diverse set of agricultural residues.

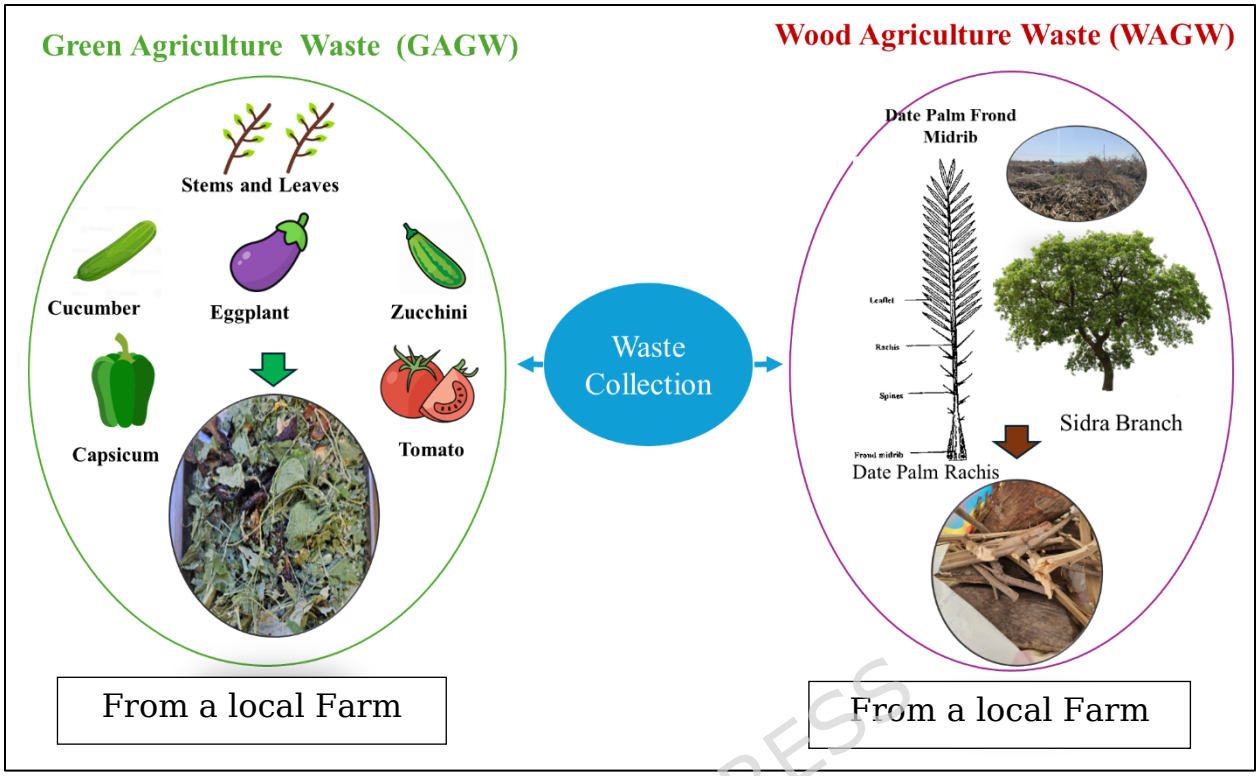

Fig. 1. Feedstocks were collected from local farms.

Table 1 presents a comparative overview of the 11 biomass feedstocks utilized in this study for biochar production. The samples are categorized into two groups: GAGW (Samples 1–7), comprising vegetables, and processed organic matter; and WAGW (Samples 8–11), consisting of tree-derived materials such as date palm frond midrib, Sidra branches, and rachis. The table highlights key characteristics of each feedstock, including physical form, estimated MC based on visual assessment, and observations from the grinding process. This classification provides insight into the inherent variability among feedstocks and the operational considerations required for their preparation. Such differences play a crucial role in influencing pyrolysis

behavior, biochar yield, and suitability for specific applications, underscoring the importance of detailed feedstock assessment in biochar research.

The decision to pool individual feedstock into two representative composite groups was driven by both practical and scientific considerations. In real agricultural settings, waste streams are inherently heterogeneous and mixed; valorization strategies must therefore be designed for aggregated fractions rather than isolated materials. Moreover, the individual physicochemical properties of the constituent biomass types, including date palm fronds, Sidra branches, and common vegetable residues are well-documented in the literature. Grouping by biomass category (green/herbaceous vs. woody/lignocellulosic) is consistent with established classification frameworks and allowed for meaningful comparison of two fundamentally distinct biochemical compositions under identical pyrolysis conditions.

Table 1. Biomass feedstocks used for biochar production. Composite samples (Samples 7 and 11, highlighted in bold) represent the mixed fractions selected for systematic pyrolysis and characterization, reflecting the heterogeneous nature of real agricultural waste streams.

Groups	Sample No.	Feedstock	Category	Form	MC (%)	Grinding Notes
Green agricultural waste (GAGW)	1	Eggplant-fresh waste	Vegetable	Thin dried slices	93.87	Smooth grind, minimal resistance
	2	Zucchini-fresh waste	Vegetable	Sliced and dried	92.95	Easy to handle and grind
	3	Tomatoes-fresh waste	Vegetable	Sticky dried pieces	92.85	Sticky residue

	4	Cucumber-fresh waste	Vegetable	Thin dry chips	96.39	Similar to zucchini
	5	Capsicum-fresh waste	Vegetable	Wrinkled, dried skin	91.23	Lightweight, easy to powder
	6	Green leaves and stems-fresh waste	Plant Matter	Fibrous dried parts	83.25	Slightly fibrous, but grinds well
	7	**Mixed Agricultural Waste (1-6)**	**Composite / Processed**	**Pre-ground mixture**	**87.75**	**Easy grinding, fine powder**
Woody agricultural waste (WAGW)	8	Dried* date Palm Frond Midrib	Woody Agricultural Waste	Rigid stem segment	9.06	Tough fiber, needs coarse grinding
	9	Dried sidra Branch	Woody Agricultural Waste	Thin woody twigs	7.44	Dry and woody; moderate grinding effort
	10	Dried date Palm Rachis	Woody Agricultural Waste	Fibrous central stalk	6.98	Dense core, requires powerful grinding
	11	**Mixed Woody Agricultural Waste (8-10)**	**Blended / Composite**	**Mixing woody feedstocks**	**7.83**	**Fine ground**

*Naturally sun-dried on the farm. **Note**: Moisture content (MC) values reported in this table reflect the initial as-received condition of each feedstock prior to laboratory pre-treatment. All feedstocks were subsequently oven-dried at 105°C for 8 hours under standardized laboratory conditions prior to pyrolysis to eliminate residual MC and ensure experimental reproducibility.

2.2. Feedstock samples preparation

Initial pre-treatment involved the removal of physical contaminants, after which the cleaned wastes were bagged and clearly labelled for identification and traceability. Each waste type was weighed before and after drying using a Binder ED23 heating oven at 105 ℃ for 8 h to determine MC (%)[38,39]. Following drying, each waste type was individually grounded using a mechanical grinder (IKA M20 Universal Mill) and sieved (0.25 mm) to produce a uniform and fine particle size ≤ 0.25 mm suitable for pyrolysis and characterization. The ground materials were then stored in labeled containers to maintain sample integrity.

2.3. Pyrolysis Procedure

Pyrolysis experiments were conducted using an SH Scientific SH-FU-18.7MHV furnace (18.7 L capacity, maximum temperature of 1500 °C; SH Scientific Co., Ltd., Sejong, South Korea), equipped with a mass flow controller, back pressure regulator, digital vacuum gauge, and vacuum pump, under controlled inert conditions. A constant heating rate of 5 °C/min was applied in all experiments, in accordance with the manufacturer's recommended operating conditions for stable and uniform thermal decomposition. The system was heated from ambient temperature to the target temperature (300–600 °C), followed by an isothermal holding period (20–120 min), and then allowed to cool naturally to room temperature while maintaining continuous nitrogen flow (0.2L/min). The nitrogen flow rate (0.2 L/min) was selected based on the small sample mass (~3 g) and reactor volume. This flow rate is sufficient to maintain oxygen-free conditions by

continuously purging volatile products and preventing oxidative reactions. Similar flow rates (0.1–0.5 L/min) are commonly reported for laboratory-scale fixed-bed pyrolysis systems, where excessive flow is avoided to prevent heat loss and unnecessary gas consumption while still ensuring an inert environment [40].

All feedstocks were dried, ground, and sieved to a particle size of approximately 0.25 mm to ensure uniform heat transfer and reproducibility. The sample mass used in each experiment was approximately 3 g, which is appropriate for the furnace capacity and ensures consistent thermal behavior.

The reactor operates as a batch-type fixed-bed system, where gas residence time is governed by the nitrogen flow rate and reactor geometry. Due to the small sample size and continuous purge, secondary reactions are minimized and volatile products are efficiently removed.

All experiments were conducted in duplicate, and the reported results represent averaged values to ensure reproducibility and reliability.

To facilitate tracking and identification, each sample was assigned a unique code (e.g., BC-3-60-1), as illustrated in Fig. 2. Experimental settings for producing biochar from GAGW and WAGW via pyrolysis are shown in Fig. 3, Fig. S1 and S2.

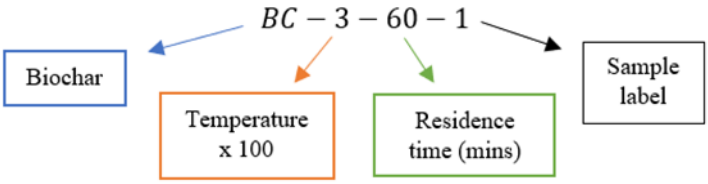

Fig. 2. Biochar samples abbreviation.

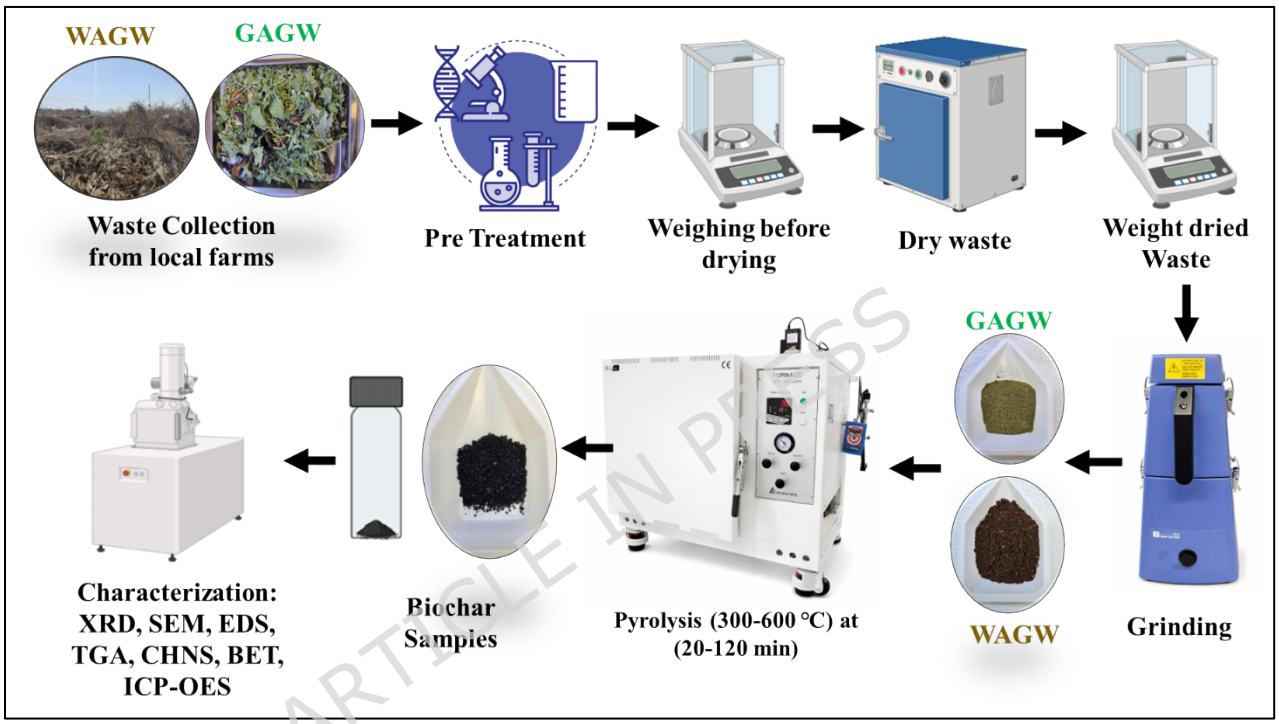

Fig. 3. Experimental setup for producing biochar from green agricultural waste (GAGW) and woody agricultural waste (WAGW) collected from a local farm in Qatar via pyrolysis.

2.4 Samples Characterization

2.4.1. Thermogravimetric Analysis

Thermogravimetric analysis (TGA) was performed on a TA Instruments Discovery TGA. Approximately 10 ± 0.5 mg of each sample was loaded into a tared platinum pan. Each sample was analyzed twice: once under a 100%

nitrogen atmosphere (Grade 5) and once under a 70/30 nitrogen/oxygen mixture (both Grade 5), with a constant purge gas flow rate of 50 mL/min for both runs. All samples were heated from 40 °C to 1000 °C at a ramp rate of 5 °C/min.

2.4.2. Proximate and Yield Analysis

Moisture content (MC), ash, volatile matter (VM), and fixed carbon (FC) contents in the biochar samples were determined following American Standard Testing and Materials (ASTM) D1762-84 Standard [38,39] and TGA data. Approximately 1 g of ground sample (0.25mm sieve) was used for the test, and all crucibles were pre-heated at 105 °C for 2 hours and cooled in a desiccator before weighing. MC (%) was measured by heating the sample into an open crucible at 105 °C for 8 h in a box muffle furnace (Thermo Scientific-Thermolyne), followed by cooling in a desiccator for 1 h and reweighing . The mass loss due to evaporation represents the moisture content. Volatile matter (%) was determined by placing the previously dried sample in a covered crucible and heated it rapidly to 950 °C for 6 min in the muffle furnace. The weight loss during this step corresponds to the VM released from the sample. Ash (%) was measured by transferring the residue to an uncovered crucible and burning it at 750 °C in the muffle furnace for 6 h under air. Cool the crucibles with lids in place in a desiccator for 1 h and weigh. The mass of material remaining after burning is called ash.

The FC (%), and yield concentration were determined by the following Equations:

$$FC\ (\%) = 100 - (VM\ (\%) + Ash\ (\%)) \quad (1)$$

$$Yield\ (\%) = \left(\frac{\text{biochar mass}}{\text{105℃ dried biomass}}\right) x100 \quad (2)$$

All measurements were performed in duplicate using an analytical balance with 0.1 mg precision, and results were reported to be at the nearest 0.05%.

2.4.2. 1 Proximate Measurements from TGA data

Volatile matter was also determined using TGA under an inert nitrogen (N_2) atmosphere. The sample was heated from ambient temperature to 600 °C at a controlled heating rate, and the mass change was continuously recorded. MC was first quantified as the mass loss occurring up to 105 °C under N_2. Following moisture removal, VM was defined as the mass loss associated with thermal devolatilisation of non-aqueous organic components in the absence of oxygen.

In this study, VM was also calculated as the mass loss occurring between 105 °C and 600 °C under N_2. Ash content was determined separately as the residual mass remaining at 900 °C under an oxidative (O_2) atmosphere to ensure complete combustion of the remaining carbonaceous material. Fixed carbon was calculated by difference using the mass remaining at 600 °C under N_2 after subtracting the ash fraction.

The proximate analysis parameters were calculated according to the following Equations:

$$MC = 100 - W_{105,N_2} \quad (3)$$

$$VM = W_{105,N_2} - W_{600,N_2} \quad (4)$$

$$\text{Ash} = W_{900,O_2} \quad (5)$$

$$\text{FC} = W_{600,N_2} - \text{Ash} \quad (6)$$

where W_T represents the percentage mass remaining at temperature T.

2.4.3. Physicochemical Characterization

Biochar pH and electrical conductivity (EC) were measured using a Thermo Scientific Orion Versa Star Pro pH meter and a Thermo Scientific Orion Star A212 conductivity meter, respectively, at a 1:20 (w/v) biochar-to-deionized-water ratio. The specific surface area was determined by N_2 adsorption using the Brunauer–Emmett–Teller (BET) method (Micromeritics ASAP 2020 surface area analyzer, Georgia, USA) after degassing the samples at 200 °C for 8 h.

2.4.4. Ultimate and Heavy Metal Analysis

The carbon (C), hydrogen (H), nitrogen (N), and sulfur (S) composition of the samples was determined using a Flash 2000 organic elemental analyzer (ThermoScientific, Waltham, MA, USA). Each analysis was performed on approximately 3.5 mg of sample on a dry, ash-free basis.

Total oxygen content (O%) was calculated by difference, based on the following formula:

$$O\% = 100 - \text{Ash}\% - C\% - N\% - H\% - S\% \quad (7)$$

Approximately 0.1 g of each dried feedstock and biochar sample was processed using microwave-assisted acid digestion (CEM MARS 6, Matthews, NC, USA). Each sample was digested at 200°C in 8 mL of a 7:1 (v/v) solution of concentrated nitric acid (HNO_3) and hydrochloric acid (HCl). Following

digestion and appropriate dilution, the concentrations of 31 target metals were measured by Inductively Coupled Plasma-Optical Emission Spectrometry (ICP-OES; Agilent 5800, Santa Clara, CA, USA), with typical instrument detection limits of 1–50 µg/L. Consequently, elemental concentrations reported as <0.1 mg/kg in Table 8 indicate that measured values fell below this analytical detection threshold and should not be interpreted as absolute absence of the element.

2.4.5. Structural and Morphological Analysis

Crystalline mineral phases were identified by X-ray diffraction using a Bruker D8 Advance diffractometer with Cu-Kα radiation over a 2θ range of 10°–80°. Surface morphology and microstructural features were examined using a field emission scanning electron microscope (FE-SEM), QUANTA FEG 650 (Thermo Fisher Scientific, USA). X-ray fluorescence analysis (XRF, Rigaku Sequential , Japan) was used to determine the elemental composition of the biomass samples. Dried and finely ground samples were analyzed using an XRF spectrometer under standardized operating conditions.

2.5 Data Analysis

Data were processed and visualized in Microsoft Excel and Origin 2020. Descriptive statistics are reported as mean ± standard deviation. To assess statistically significant differences in biochar properties between the two feedstock groups (GAGW and WAGW), one-way ANOVA was performed using JASP (Version 0.95) at a 95% confidence interval. Data were pooled by feedstock type across pyrolysis conditions, as the primary objective was to

characterize inherent differences between the two biomass categories. Levene's test was used to verify equality of variances prior to comparison; where this assumption was not met ($p < 0.05$), Welch's t-test was applied. Differences were considered statistically significant at $p < 0.05$.

3. Results and Discussion

3.1. Feedstock Analysis

3.1.1. XRF analysis of GAGW and WAGW

X-ray fluorescence (XRF) analysis highlights pronounced differences in the inorganic composition of GAGW and WAGW, as shown in Table 2. GAGW exhibits a nutrient-rich ash profile, with major contributions from K_2O (12.6 wt%), CaO (9.47 wt%), P_2O_5 (1.61 wt%), MgO (0.92 wt%), and measurable SO_3 and Cl. This composition is characteristic of plant-based agricultural residues and aligns with earlier findings for nutrient-rich biomass such as coffee husk biomass, rice husk, and mixed crop residues, all of which exhibit elevated K, Ca, and P contents in their ash fraction [41,42]. Such high-ash biochar derived from Ca- and K-rich biomass have been reported in the literature to exhibit potential as mineral fertilizer supplements, with the capacity to improve cation-exchange properties and soil nutrient retention [43].

The lower loss on ignition (LOI) (70.8 wt%) further confirms a higher mineral-to-organic ratio in GAGW compared with woody biomass. In contrast, WAGW has much lower mineral content, with total oxides barely exceeding 3–4 wt% and a very high LOI (96.2 wt%), indicating that woody agricultural residues are predominantly carbonaceous with minimal ash. This chemical

pattern is consistent with typical wood-derived biochar reported in the literature, which generally show low ash, high fixed carbon, and reduced concentrations of basic oxides [43,44]. Such biochar is widely recognized for its stability, high aromatic carbon content, and long-term carbon sequestration potential. Upon pyrolysis, these oxides signatures become further concentrated in the biochar. GAGW-derived biochar retains high levels of K, Ca, and P, making it function as a slow-release, multi-nutrient soil amendment. Similar K–P–Ca-rich biochar and ashes have been proposed as alkaline fertilizers, liming agents, and soil conditioners in agricultural applications [45,46]. However, the relatively high chlorine content (1.84 wt%) must be considered, as it may impact soil salinity and corrosion processes.

The very low mineral content and high carbon purity of WAGW-derived biochar suggest potential suitability for applications requiring high porosity and structural stability, such as pollutant adsorption, soil structure improvement, or long-term carbon sequestration, though direct application performance remains to be validated experimentally. These properties match those reported for wood-derived biochar used in the removal of toxic elements from water and wastewater, environmental remediation, and soil enhancement [44,47]. Together, the XRF results indicate a complementary role for the two feedstocks: GAGW is a promising precursor for nutrient-rich, ash-active biochar and fertilizer or liming products, while WAGW is better suited for high-carbon, structurally stable biochar targeted at soil conditioning and environmental remediation.

Importantly, these compositional divergences are fully consistent with the anticipated behavior of the individual constituent biomass types comprising each composite group, as established in the broader literature. The elevated K_2O, CaO, and P_2O_5 content of GAGW reflects the well-documented nutrient-rich ash profiles of vegetable and leafy residues, while the high LOI and minimal oxide fraction of WAGW mirrors the low-ash, carbon-dominant chemistry characteristic of date palm and woody lignocellulosic feedstocks[43,44]. This agreement between the mixed composite results and the expected individual feedstock behavior validates the representativeness of the pooled groups and confirms that the mixing strategy did not introduce confounding effects on inorganic composition.

Table 2. XRF analysis of green agricultural waste (GAGW) and woody agricultural waste (WAGW).

No.	Component-GAGW	GAGW (wt%)	Component-WAGW	WAGW (wt%)
1	Na_2O	0.185	Na_2O	0.133
2	MgO	0.920	MgO	0.244
3	Al_2O_3	0.0231	Al_2O_3	0.0144
4	SiO_2	0.658	SiO_2	0.413
5	P_2O_5	1.61	P_2O_5	0.116
6	SO_3	1.56	SO_3	0.330
7	Cl	1.84	Cl	0.685
8	K_2O	12.6	K_2O	1.160
9	CaO	9.47	CaO	0.669
10	MnO	-	MnO	0.0026
11	Fe_2O_3	0.104	Fe_2O_3	0.0140
12	NiO	0.0297	ZnO	0.0010
13	Br	0.0180	Br	0.0030
14	SrO	0.218	SrO	0.0131
15	LOI*	70.8	LOI	96.20

*LOI is loss on ignition

3.2. XRD of biomass and biochar

Biochar samples produced at higher temperatures (500-600 °C) and longer residence time (120 min) were selected for XRD study because these conditions yielded the highest surface area and most developed structure, making them the most representative samples for advanced characterization.

Fig. 4 shows XRD patterns of the raw biomasses (GAGW and WAGW) and the derived biochar produced at 500–600 °C for 120 min reveal a predominantly amorphous carbon matrix superimposed with distinct crystalline mineral phases originating from the inorganic ash fraction. All samples exhibit a broad diffraction halo centered at 2θ approximately 22–25°, assigned to turbostratic/disordered carbon domains, confirming limited graphitization even at the highest pyrolysis temperature. Superimposed on this background, sharp reflections indicate the presence of thermally stable mineral phases. The dominant crystalline phase in all biochar is calcium carbonate (calcite), identified by its intense (104) reflection at 2θ ≈ 29.4°, together with secondary reflections at ~23.0, 35.9, 39.4, 43.1, and 47- 49°, in excellent agreement with reference calcite patterns (PDF 01-086-2334, 01-083-4602, and 01-078-3262). Potassium chloride (sylvite) is clearly detected by its characteristic cubic reflections at 2θ ≈ 28.3° (200), 40.5° (220), 50.2° (222), and 58.6°(400), corresponding to PDF No. 00-041-1476, indicating significant concentration and recrystallization of K-bearing salts during pyrolysis. Disordered carbon is further supported by weak reflections near 22.7° and 26.6° (PDF No. 00-050-0926), while sodium oxalate (natroxalate,

PDF No. 04-013-1750) is detected mainly in WAGW-derived samples through reflections at about 30.8-31.6° and 34-35°, suggesting incomplete decomposition or secondary salt formation. In selected biochar (e.g., BC-5-120-11), minor reflections attributable to calcium silicon phosphide ($Ca_3Si_2P_4$, PDF No. 04-021-8537) are observed, indicating mineral reorganization and solid–state reactions among Ca-, Si-, and P-rich ash components under reducing pyrolytic conditions. Crystallite sizes estimated using the Scherrer equation applied to the most intense peaks produce values of approximately 45-65 nm for calcite (104) and 70-95 nm for sylvite (200), confirming the presence of relatively coarse, well-crystallized mineral domains embedded within an amorphous carbon framework. From a Rietveld-style semi-quantitative perspective, although full refinement was not performed, relative peak intensities and phase persistence across samples indicate that calcite constitutes the major crystalline fraction, followed by sylvite, with carbon contributing predominantly as an amorphous phase and natroxalate and $Ca_3Si_2P_4$ present only as minor constituents. The sharpening and intensity increase of calcite and KCl peaks with increasing pyrolysis severity suggest mineral concentration and recrystallization due to organic matter volatilization rather than new carbonate formation. It is clear that the coexistence of a disordered carbon matrix with stable alkaline mineral phases ($CaCO_3$ and KCl) is expected to strongly influence the surface chemistry, alkalinity, and ion-exchange behavior of the biochar, which is highly relevant for water treatment and environmental remediation applications [48]. Phase

summary and calculated crystallite size was listed in Table S1 (see supplementary data).

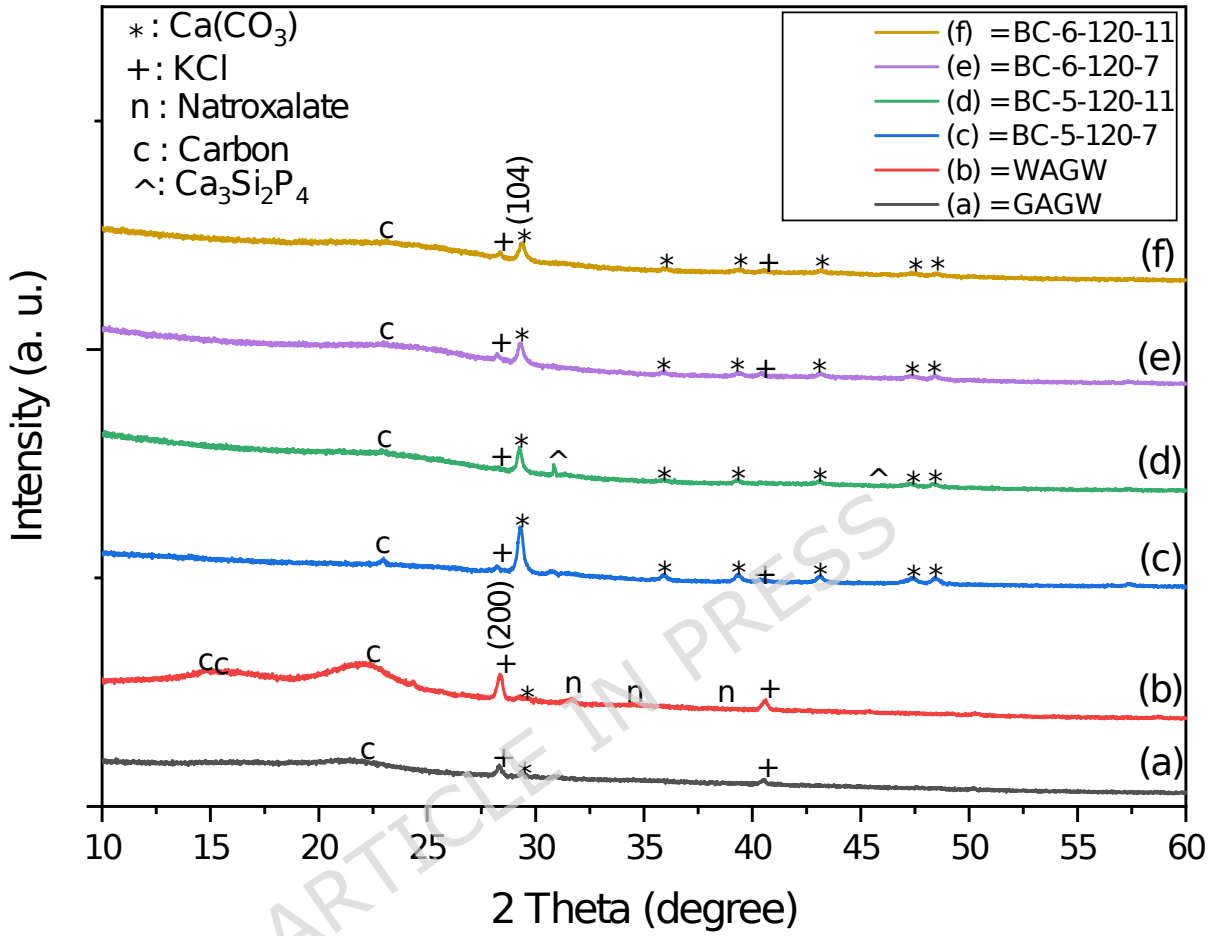

Fig. 4. XRD patterns of the raw biomasses green agricultural waste (GAGW)and woody agricultural waste (WAGW) and the derived biochar produced at 500–600 °C for 120 min.

3.3. pH and electrical conductivity (EC) of biomass and biochar samples

The pH and electrical conductivity (EC) values of the raw biomass and resulting biochar samples show a clear thermochemical progression associated with increasing pyrolysis severity (temperature and time) as displayed in Fig.5 and Table S2 (see supplementary data). The raw biomass,

GAGW and WAGW, show near-neutral to slightly acidic pH values (7.0 and 5.1, respectively) and moderate EC levels (6.17 and 4.29 mS/cm), reflecting their inherent organic acid composition and relatively low concentrations of soluble mineral ions. Following pyrolysis at 300°C for 60 minutes, the BC-3-60-7 and BC-3-60-11 biochar show a modest increase in alkalinity (pH 7.47–9.30) and EC (5.09–5.19 mS/cm), indicating partial decomposition of weak acidic oxygen-containing functional groups and the early mobilization of mineral salts. A more pronounced shift is observed in the biochar produced at 600°C (BC-6-60-7 and BC-6-60-11), where substantial increases in both pH (7.96-10.79) and EC (10.05-13.50 mS/cm) demonstrate intensified carbonization, ash enrichment, and the formation of basic mineral phases such as carbonates and oxides as conformed by XRD and EDS analysis. Extending the residence time at 600°C to 120 minutes (BC-6-120-7 and BC-6-120-11) further elevates pH (10.83–12.36) while producing slightly lower EC values (8.36–10.83 mS/cm), suggesting increased structural stabilization and partial immobilization of soluble inorganic constituents as pyrolysis progresses. These thermal-response patterns are fully consistent with previous studies reporting progressive increases in pH and EC with rising pyrolysis temperature due to the loss of acidic functionalities and concentration of inorganic ash components [49-51], confirming the systematic transition from raw biomass to highly carbonized, mineral-rich biochar. *Li et al.*[52] reported that biochar pH and EC are mainly controlled by its chemical functional groups. In rice straw biochar, both pH and EC are governed by

fused-ring aromatic structures and anomeric O-C-O carbons. In rice bran biochar, pH is influenced by both aromatic structures and aliphatic O-alkyl (HCOH) groups, indicating that different feedstocks retain different functional groups that regulate the alkalinity and conductivity of the resulting biochar.

When pooled by feedstock group across all pyrolysis conditions, mean pH was slightly higher for GAGW-derived biochar (10.02 ± 0.71) compared to WAGW-derived biochar (9.70 ± 1.93), though this difference was not statistically significant ($p = 0.799$); similarly, EC was higher for GAGW (10.35 ± 4.51 mS/cm) than WAGW (7.14 ± 1.78 mS/cm) but did not reach statistical significance ($p = 0.315$), suggesting that while GAGW consistently trends toward higher ionic activity, the considerable within-group variation across pyrolysis conditions moderates the between-group contrast.

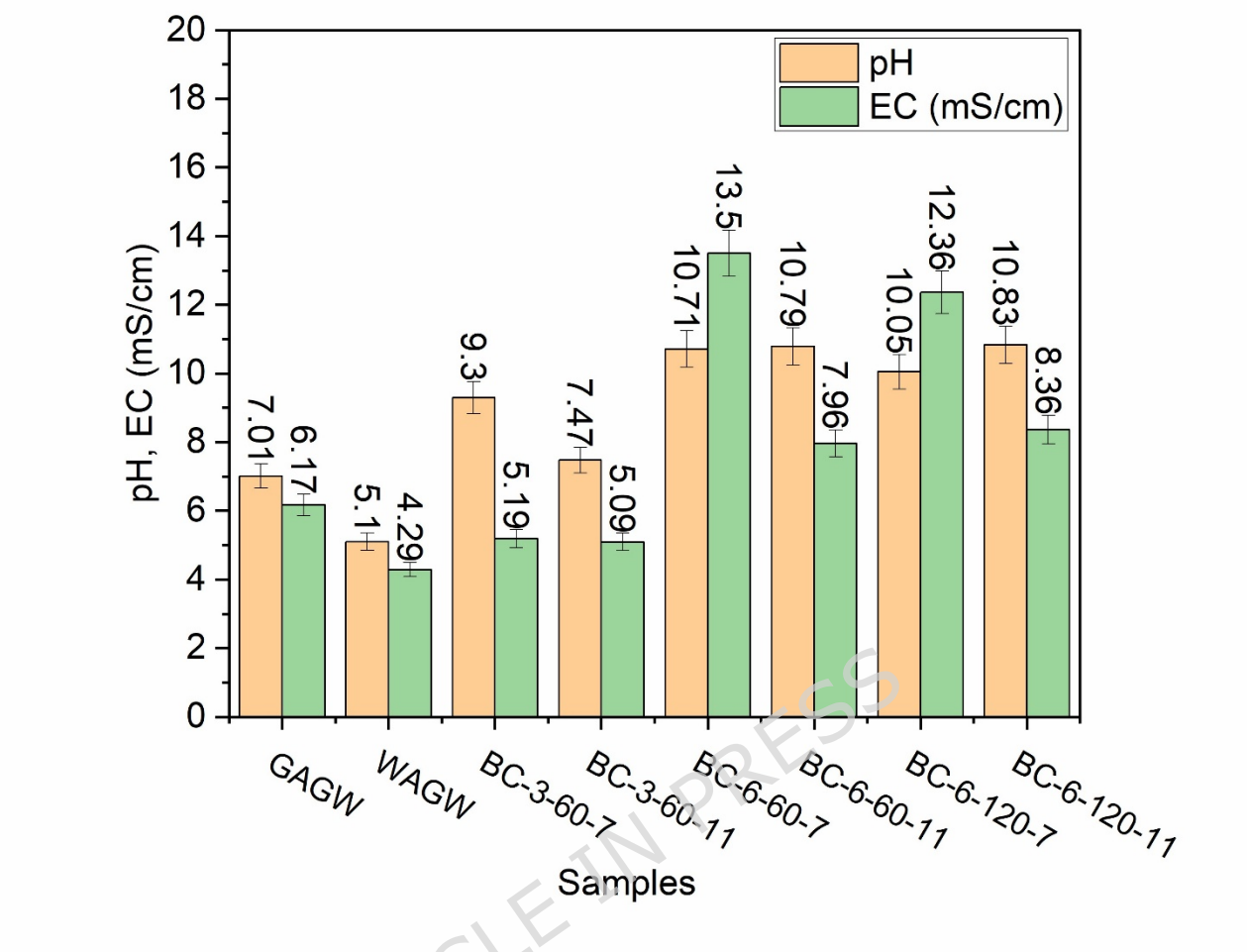

Fig. 5. pH and electrical conductivity of biomass and biochar samples.

3.4. TGA analysis of GAGW and WAGW

Fig. 6 displays the TGA analysis of GAGW (a and b) and WAGW (c and d) feedstocks from 40 to 1000 ℃ under N_2 and O_2 flow. The 10% weight loss at about 105 °C is related to the removal of moisture. However, the weight loss observed between 100 and 400 °C, is due to the decomposition of organic compounds [53]. Finally, the weight loss observed above 600 °C is mainly due to the conversion of cellulose and hemi-cellulose into more stable carbon forms and the partial decomposition of inorganic compounds as also reported in other studies. Cellulose is the most extensively studied and best

understood among the three main biomass components: cellulose, hemicellulose, and lignin. According to the widely accepted Waterloo mechanism, cellulose pyrolysis proceeds through a series of competitive reactions, including dehydrogenation, depolymerisation, and fragmentation, each becoming dominant within specific temperature ranges [54]. TGA revealed that hemicellulose undergoes maximum degradation between 185 and 325℃, cellulose between 270 and 400℃, and lignin between 200 and 500℃ [55]. Consequently, raised temperatures lead to an augmented degradation of these components, leading to decreased biochar yield. The moisture, volatile matter content, ash, fixed carbon and biochar yield produced from the feedstocks can be accurately determined from TG analysis which is called TGA-based proximate analysis method [56-58]. The calculated proximate analysis of GAGW and WAGW from TGA data is shown in Table 3.

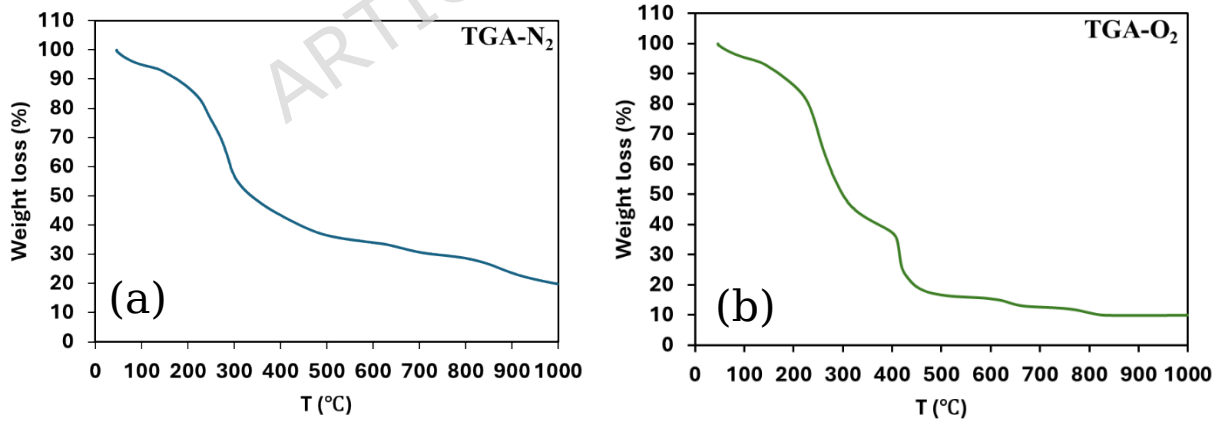

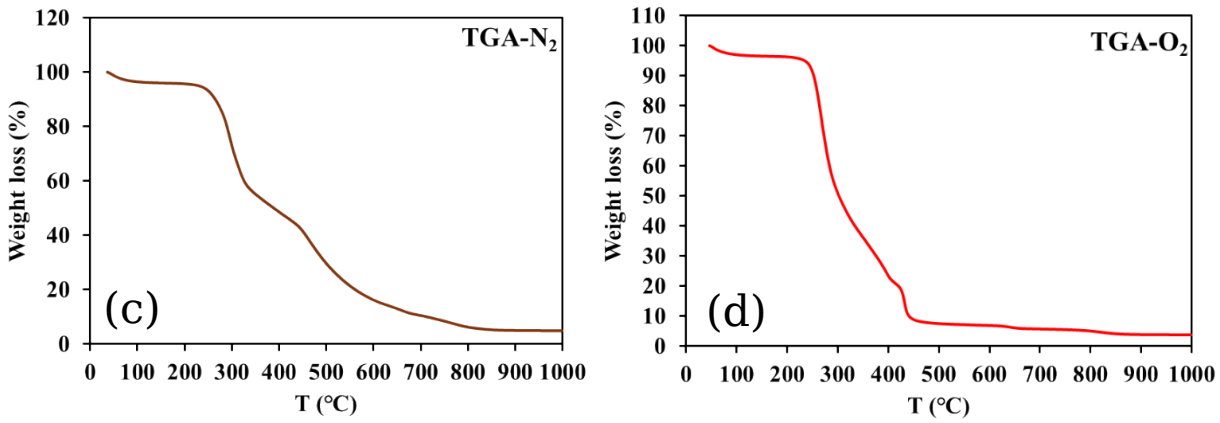

Fig. 6. TGA analysis of green agricultural waste (GAGW) (a and b) and woody agricultural waste (WAGW) (c and d).

Table 3: Proximate analysis of green agricultural waste (GAGW) and WAGW from TGA data.

Sample on a dry basis	MC (db)* (wt.%)	VM (wt.%)	FC (wt.%)	Ash (wt.%)
GAGW	4.2	62.3	23.5	10
WAGW	3.32	77.98	14.70	4

*(db) dry basis under the sun

3.5. Morphological, Structural, and Elemental Analysis

Fig. 7 shows SEM images of WAGW biochar produced at 600 °C for 120 min (5 °C min^{-1}, N_2 0.2 L min^{-1}), which exhibited a more fibrous, layered microstructure with potential for a high surface area 680 m^2/g with more porous. EDS analysis of WAGW biochar had high carbon (82.62 atom%) and (11 atom%) oxygen and traces (Na, Mg, Si, Ca, P, S, Cl, K and Al). The SEM and EDS results reveal a carbonized plant-tissue framework with longitudinal channels and ribbed walls that preserve the original xylem/fiber architecture, providing continuous macropore pathways; higher magnifications show rough, lamellar carbon domains with slit-type voids and micro-fractures

formed by devolatilization, consistent with entrances to meso/micropores (the latter not directly resolved by SEM). Bright, electron-dense particulates anchored on the surface are frequent and correspond to mineral ash inclusions that partly decorate and locally obstruct pore mouths. EDS (semi-quantitative) indicates a carbon-rich matrix (C = 71.94 mass %) with residual oxygen (O 12.84 mass %) implying surface oxygenated functionalities (e.g., –OH/–COOH/C=O), together with appreciable alkali/alkaline-earths and siliceous phases (K = 4.80, Ca = 2.83, Cl = 2.70, Mg = 1.83, Si = 1.72, Na = 0.76, S= 0.45, Al = 0.08, P = 0.06 = mass %), which appear as the bright particles; hydrogen is not detected by EDS and oxygen quantification is approximate. The moderate heating rate and long hold promote gradual volatile release, mitigate structural collapse, and allow migration/sintering of these minerals (e.g., K/Ca/Mg salts, carbonates, and phytolithic silica), which can catalyze in-situ activation and increase basicity but may require post-washing to minimize leachable ions (notably Cl, K, Na) and pore blockage. The material exhibits a hierarchical pore system (macro-channels feeding smaller pores) and a largely aromatic carbon backbone with oxygenated sites and basic ash domains.

Fig. 8 shows the SEM micrographs and corresponding EDS spectra of GAGW-derived biochar produced at 600 °C for 120 min under an N_2 atmosphere (0.2 L min^{-1}) with a heating rate of 5 °C min^{-1}. The SEM images reveal a well-developed porous and heterogeneous carbon matrix, indicating extensive devolatilization and structural rearrangement at high pyrolysis

temperature, which is favorable for adsorption-related applications. The EDS analysis confirms that carbon (73.11% atom%) and oxygen (20.41% atom%) are the dominant elements, accompanied by inorganic constituents such as K, Ca, Si, Al, P, S, Cl, Na and Mg, originating from the intrinsic ash content of the feedstock. The homogeneous distribution of these mineral elements suggests their incorporation within the carbon matrix, which may influence surface reactivity, alkalinity, and potential catalytic or adsorption behavior of the biochar.

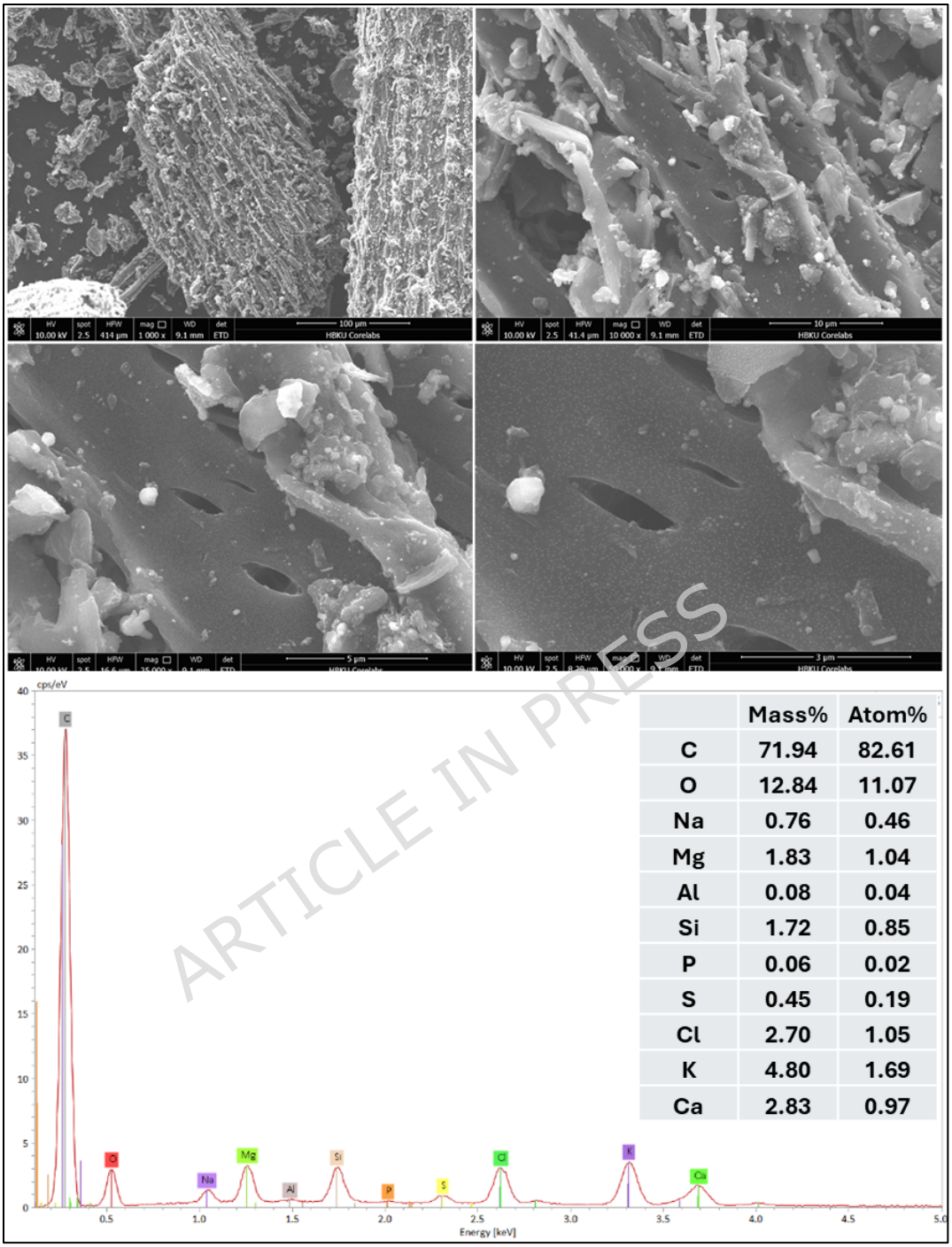

	Mass%	Atom%
C	71.94	82.61
O	12.84	11.07
Na	0.76	0.46
Mg	1.83	1.04
Al	0.08	0.04
Si	1.72	0.85
P	0.06	0.02
S	0.45	0.19
Cl	2.70	1.05
K	4.80	1.69
Ca	2.83	0.97

Fig. 7. SEM images and EDS analysis of woody agricultural waste (WAGW) biochar pyrolyzed at 600 ℃ for 120min, HR ℃ 5/min and N_2 (0.2L/min).

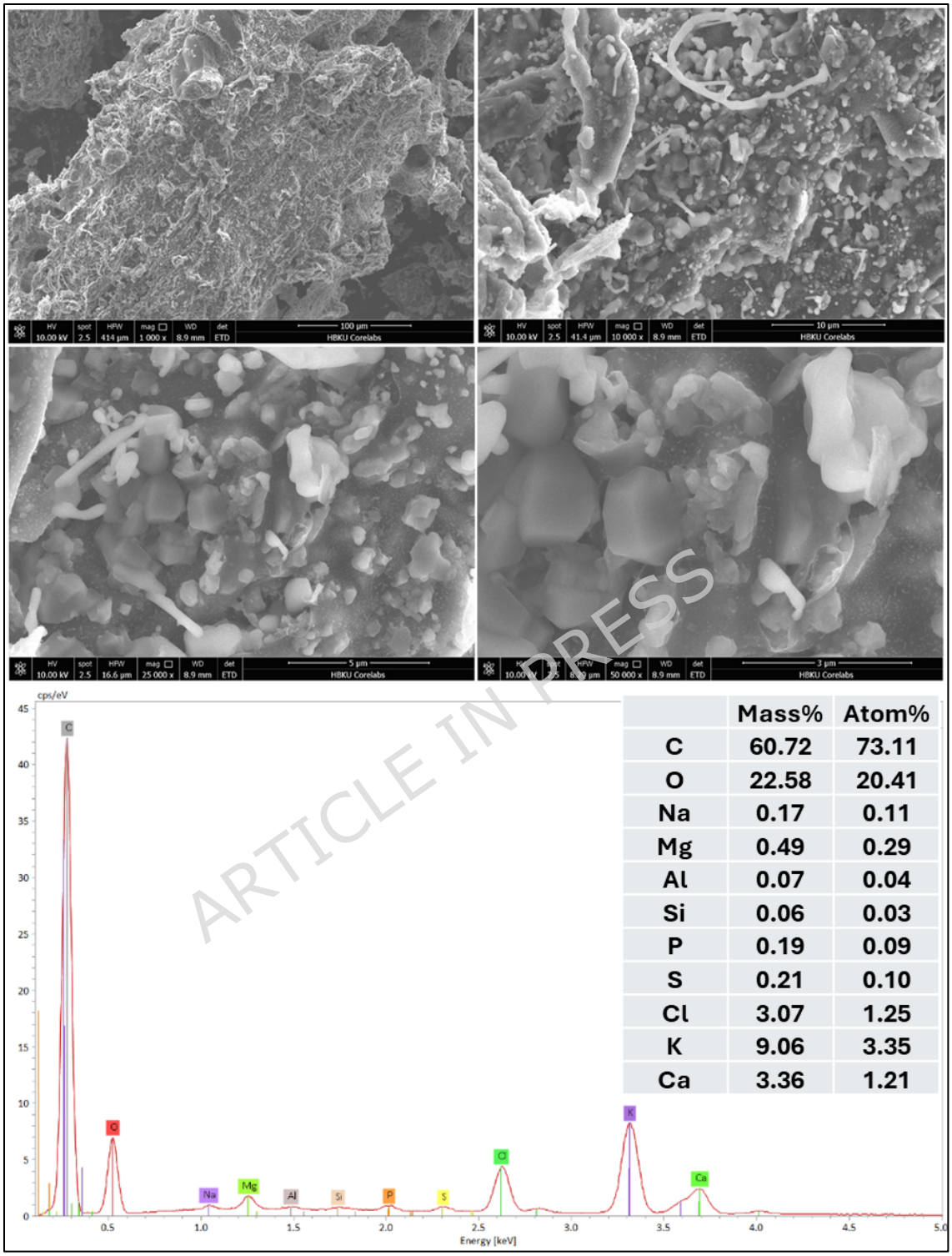

	Mass%	Atom%
C	60.72	73.11
O	22.58	20.41
Na	0.17	0.11
Mg	0.49	0.29
Al	0.07	0.04
Si	0.06	0.03
P	0.19	0.09
S	0.21	0.10
Cl	3.07	1.25
K	9.06	3.35
Ca	3.36	1.21

Fig. 8. SEM images and EDS analysis of green agricultural waste (GAGW) biochar pyrolyzed at 600 ℃ for 120min, HR ℃ 5/min and N_2 (0.2L/min).

3.6. Effect of Pyrolysis Temperature on the Yield and BET Surface Area

Fig. 9 illustrates that the yield of biochar production from both GAGW and WAGW systematically decreases with the increase in pyrolysis temperature from 300 to 600 ℃, and to a lesser extent with the increase in residence time from 20 to 120 min. This behavior aligns with the typical volatilization pattern of lignocellulosic biomass, where hemicellulose, cellulose, and lignin gradually decompose into gases and condensable vapors, leaving a smaller portion of solid carbonaceous residues (biochar) [59-61]. At 300 ℃, only limited decomposition occurred and leaves substantial amounts of cellulose, hemicellulose, and lignin, only partially decomposed, so GAGW and WAGW show their highest yields (71-60%), similar to the high biochar yields recorded in wood and agricultural residues under mild carbonization conditions [54,62]. As the temperature rises to 400-500 ℃, the yield of both raw materials sharply decreases, reflecting the main devolatilization window of cellulose and lignin; similar decreases in the yield of softwood and hardwood, as well as green biomass such as crop residues and grasses, have been described within this range [63].

At 600 ℃, the productivity approaches a steady level, indicating the removal of most thermally unstable components, and further heating will only cause a slight loss in mass, which is consistent with the coal densification system mentioned in other studies on the slow pyrolysis of wood and forest residues [64-66]. Residence time exerts a secondary effect: extending the

residence time from 20 to 120 minutes at a specified temperature leads to a slight but consistent decrease in yield, which aligns with previous studies on the slow pyrolysis of woody and green biomass, where prolonged residence time enhances secondary cracking of vapors and allows for polymerization reactions to increase solid-phase volatiles [67]. Under all conditions, the yields of WAGW were consistently higher than the yields of GAGW, reflecting observations that indicate that woody raw materials generally produce more char and contain a higher proportion of thermally stable lignin compared to green biomass, which tend to be richer in volatile components and ash as seen in TGA analysis [63,68]. This observation was statistically confirmed: when pooled across all pyrolysis conditions, WAGW yielded significantly more biochar (50.92 ± 9.2%) compared to GAGW (42.50 ± 8.8%), a difference that was statistically significant ($p = 0.012$), reflecting the higher thermally stable lignin content of woody feedstocks relative to the more volatile-rich green biomass.

Table 4 summarizes and reviews pyrolysis operating conditions and textural properties of biochar reported in the literature.

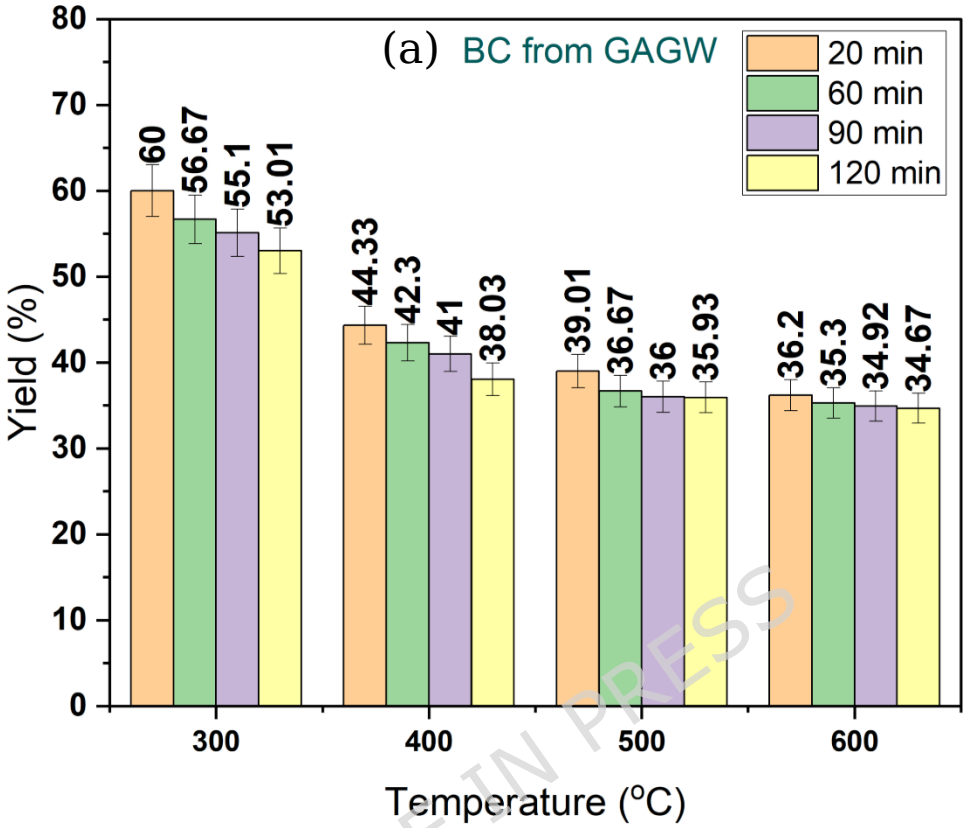

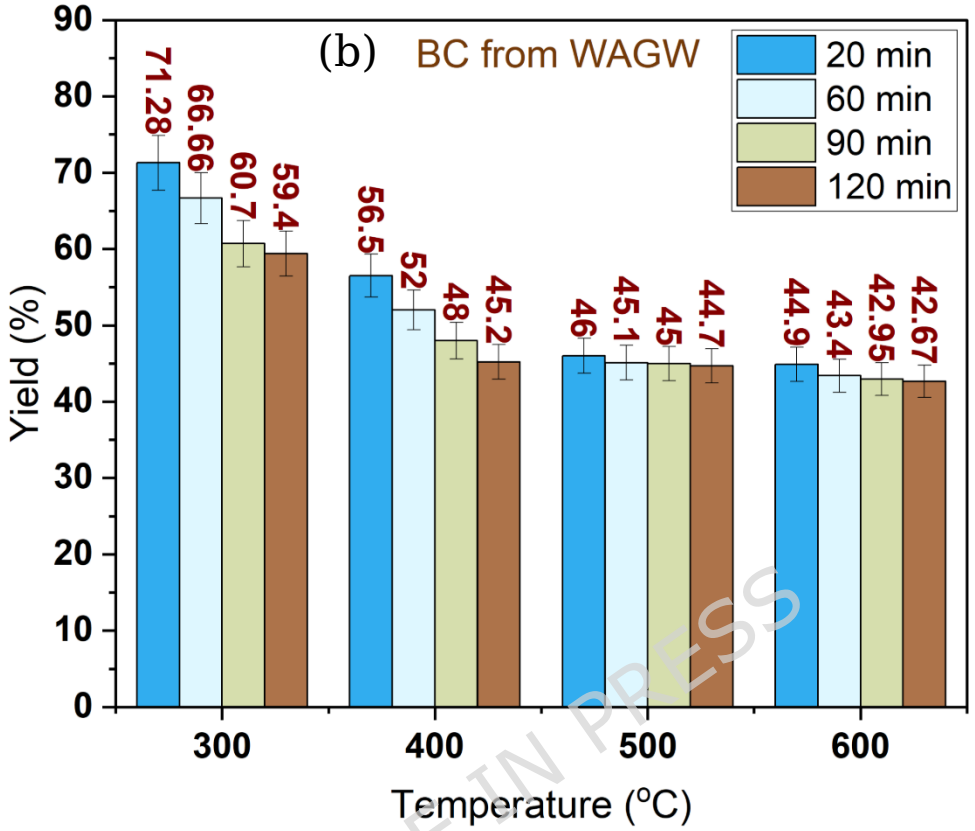

Fig. 9. Yield versus temperature at different residual times (a) BC from green agricultural waste (GAGW) and (b) BC from woody agricultural waste (WAGW).

Table 4. Pyrolysis operating conditions and textural properties of biochar reported in the literature.

Sample ID	Feedstock	Temperature (°C)	Heating Rate (°C/min)	Time (min)	Yield (%)	BET (m^2/g)	Ref.
BC700	Date Palm Waste	700	—	240	—	283.62	[69]
BC900	Date Palm Waste	900	—	240	—	291.11	[69]
DP-BC	Date Palm Fronds	400	—	—	—	6.12	[70]
Poplar Biochar	Poplar Wood	600	30	—	—	411.06	[71]

TW250	Woody Chips	250	—	30	—	—	[62]
TW275	Woody Chips	275	—	30	—	<1	[62]
TW300	Woody Chips	300	—	30	—	—	[62]
CW325	Carbonized Wood Chips	325	—	30	—	—	[62]
CW350	Carbonized Wood Chips	350	—	30	—	<1	[62]
CW375	Carbonized Wood Chips	375	—	30	—	—	[62]
RG-BC	Rhodes Grass	400	—	—	—	3.45	[70]
	Wood-derived biochar	550	2.5	120	20–23	320	[72]
	Wood-derived biochar	800	2.5	120	20–23	456	[72]
B-6-120-7	GAGW	600	5	120	34.67	238.07	This study
B-6-120-11	WAGW	600	5	120	42.67	683.88	This study

The effect of pyrolysis temperature on the BET surface area of biochar derived from WAGW and GAGW is shown in Fig. 10. The BET surface area of biochar produced from both WAGW and GAGW increased substantially with rising pyrolysis temperature, reflecting the progressive thermal degradation of hemicellulose, cellulose, and lignin and the corresponding release of volatiles that generate new pore structures. At low temperature (300 °C), both materials exhibited minimal surface development due to incomplete devolatilization and the presence of tarry residues that remain within the

pore system. As the temperature increased to 400-600 °C, extensive volatilization and secondary cracking reactions led to the removal of thermally labile compounds, resulting in significant pore enlargement and the formation of well-defined micro- and mesopores, consistent with the mechanisms described by [59,73]. It was reported that microporosity is established at about 500 °C, and further heating volatilizes the residual material that blocks the micropores [59,74]. WAGW consistently shows much higher BET surface area (348-684 m^2/g) compared to GAGW (27-238 m^2/g). The significantly higher surface area observed for WAGW compared to GAGW at all temperatures can be attributed to the inherently higher lignin content and lower ash fraction in woody biomass, which promotes a more stable carbon framework and prevents pore blockage trends. BET surface areas obtained closely align with previous findings for wood-derived biochar exhibiting surface areas up to 320-456 m^2/g at 550-800 ℃ [72] and higher than (7.68-351 m^2/g) at (300-900 ℃)[75]. Chen et al. [71] achieved a BET surface area of 411.06 m^2/g for poplar wood biochar at 600 ℃ and a heating rate of 30 ℃/min. In contrast, the lower surface areas measured for GAGW correspond well with typical values for green and herbaceous biomass. The results confirm that pyrolysis temperature is the dominant parameter controlling surface area evolution as shown in Fig. 10 and Table 5. In contrast, biomass type exerts a secondary but significant influence, with woody feedstocks consistently producing more porous, high-surface-area biochar due to their favourable biochemical composition.

These trends are entirely consistent with what would be anticipated from the individual biomass types constituting each composite group. The notably lower surface area of GAGW biochar is plausibly attributable to its inherently higher ash content, which promotes pore-mouth obstruction by inorganic particulates a mechanism directly confirmed by high-magnification SEM imaging in this study. Conversely, the high BET surface areas achieved by WAGW biochar (up to 684 m^2/g) reflect the stable lignin-rich framework of date palm and woody feedstocks, which resists structural collapse during thermal treatment and facilitates well-defined micropore formation. The clear and predictable divergence in surface area between the two composite groups therefore validates the representativeness of the mixing strategy and confirms that pooling biomass by category did not mask individual feedstock behavior. Textural properties of biochar derived from GAGW and WAGW at different pyrolysis temperatures are summarized in Table 5.

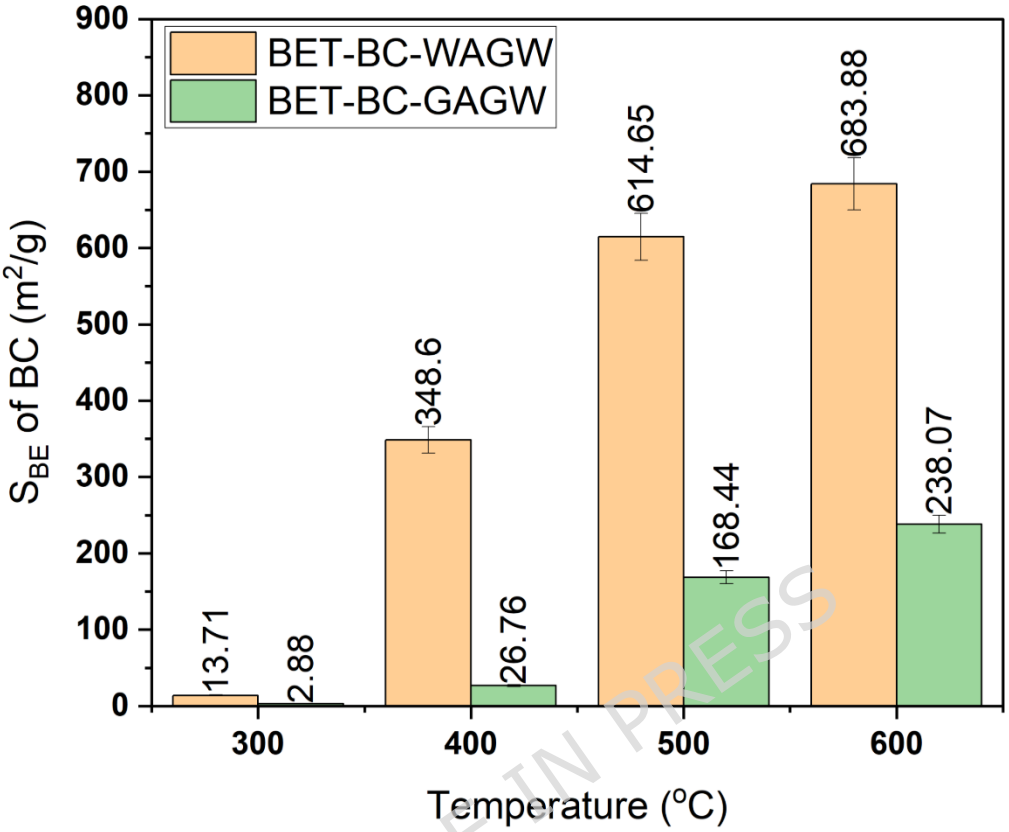

Fig. 10. BET surface area of biochar derived from woody agricultural waste (WAGW) and green agricultural waste (GAGW) at various pyrolysis temperatures.

Table 5. Summary of textural properties of biochar derived from green agricultural waste (GAGW) and woody agricultural waste (WAGW) at different pyrolysis temperatures.

Sample	Temp (°C)	BET Surface Area (m^2/g)	Micropore Area (m^2/g)	External Surface Area (m^2/g)	Micropore Volume (cm^3/g)	BJH Surface Area (m^2/g)	BJH Pore Volume (cm^3/g)	**Calculated apparent pore diameter (nm)**
B-3-120-7	300	2.88	Not reliable	Not reliable	0.0037	1.3 - 2.9	0.0037	5.1
B-4-120-7	400	26.75	Not reliable	Not reliable	0.0305	11 - 17	0.0305	4.6

B-5-120-7	500	168.44	96.71	71.73	0.0409	45.47 - 63.41	0.0789 - 0.0859	1.87- 2.04
B-6-120-7	600	238.07	221.73	16.34	0.0878	11- 12	0.0878	1.48
B-3-120-11	300	13.71	Not reliable	Not reliable	0.0241	Not detected	0.0241	7.03
B-4-120-11	400	348.6	309.74	38.85	0.1255	26- 27	0.1255	1.44
B-5-120-11	500	614.65	552.47	62.17	0.2152	38.25-47.86	0.2152	1.4
B-6-120-11	600	683.88	559.29	124.6	0.279	75.82-95.21	0.275	1.61

Notes:

- BJH surface area values reported as adsorption–desorption range
- Values where the t-plot micropore area exceeded the BET surface area were marked as not reliable and were not used for mechanistic interpretation. BJH values are reported only as mesopore range indicators because BJH analysis is less reliable for micropore dominated carbonaceous materials and may underestimate pore size in mesoporous systems [76].
- The pore diameter was estimated using the following equation [77]:

$$D_{app}\ (nm) = \frac{4000V}{S_{BET}}$$

where V is pore volume in cm^3/g and S_{BET} is BET surface area in m^2/g.

3.7. Ultimate Analysis

Elemental analysis of waste feedstocks and biochar samples is shown in Table 6. The elemental profiles of the raw feedstocks, GAGW and WAGW, were characterized to establish a baseline before pyrolysis. The carbon content was similar for both materials, with GAGW at 47.3% and WAGW at 50.0%. Upon pyrolysis, carbon content increased progressively with thermal severity for both groups, with WAGW-derived biochar achieving significantly

higher carbon enrichment (66.12 ± 5.3%) compared to GAGW-derived biochar (54.84 ± 2.6%), a difference that was statistically significant ($p = 0.009$), confirming the superior carbonization efficiency of woody lignocellulosic feedstocks. Correspondingly, ash content was significantly higher in GAGW-derived biochar (10.55 ± 2.3%) than in WAGW-derived biochar (3.90 ± 2.2%; $p = 0.006$), consistent with the mineral-dense, nutrient-rich nature of green and vegetable-based feedstocks, which inherently limits the extent of carbon densification during pyrolysis. A notable difference was also observed in nitrogen content, which was significantly higher in GAGW-derived biochar (6.69 ± 1.1%) compared to WAGW-derived biochar (1.80 ± 2.1%; $p = 0.012$), consistent with the general compositional differences between these waste types; green, leafy biomass is typically richer in proteins and other nitrogenous compounds, whereas woody biomass is primarily composed of lignocellulose [78-81]. The absence of detectable sulfur in both feedstocks is an advantageous characteristic, minimizing the potential for SO_x emissions during pyrolysis and the presence of undesirable sulfur compounds in the final product [82,83].

Fig. 11 shows the evolution of atomic H/C and O/C ratios for raw GAGW, WAGW, and their derived biochar produced under different pyrolysis temperatures (300, 400. 500, and 600 ℃) for 60 min. The raw GAGW and WAGW feedstocks exhibit relatively high H/C ratios (1.38 and 1.12, respectively) and O/C ratios (~0.50–0.58), reflecting their hydrogen- and oxygen-rich organic structures; this is consistent with the higher protein,

carbohydrate, and nitrogenous compound content typically found in green, leafy biomass, whereas woody biomass is dominated by lignocellulosic polymers with inherently lower hydrogen content [78-81]. Upon pyrolysis, both H/C and O/C ratios decrease systematically with increasing temperature and residence time, indicating progressive dehydrogenation, deoxygenation, and aromatization of the carbon matrix. Biochar produced at lower temperatures (300 ℃) retain moderate H/C values about (0.79-0.99), suggesting partial carbonization, while those produced at higher temperatures (≥ 500-600 °C) exhibit markedly lower H/C about (0.30-0.42) and O/C (< 0.24) ratios, indicative of a high degree of carbonization and the formation of condensed polycyclic aromatic structures [84]. These trends are fully consistent with previous studies reporting that biochar with H/C < 0.5 possess highly aromatic, recalcitrant structures and enhanced long-term stability in environmental applications [85-87]. Moreover, according to the European Biochar Certificate (EBC) guidelines, an H/C_{org} ratio below 0.7 is required for certified biochar, while values below 0.4 correspond to highly carbonized, long-term stable biochar; all high-temperature biochar in this study clearly satisfy these criteria, confirming their suitability for carbon sequestration, soil amendment, and advanced environmental remediation applications [24].

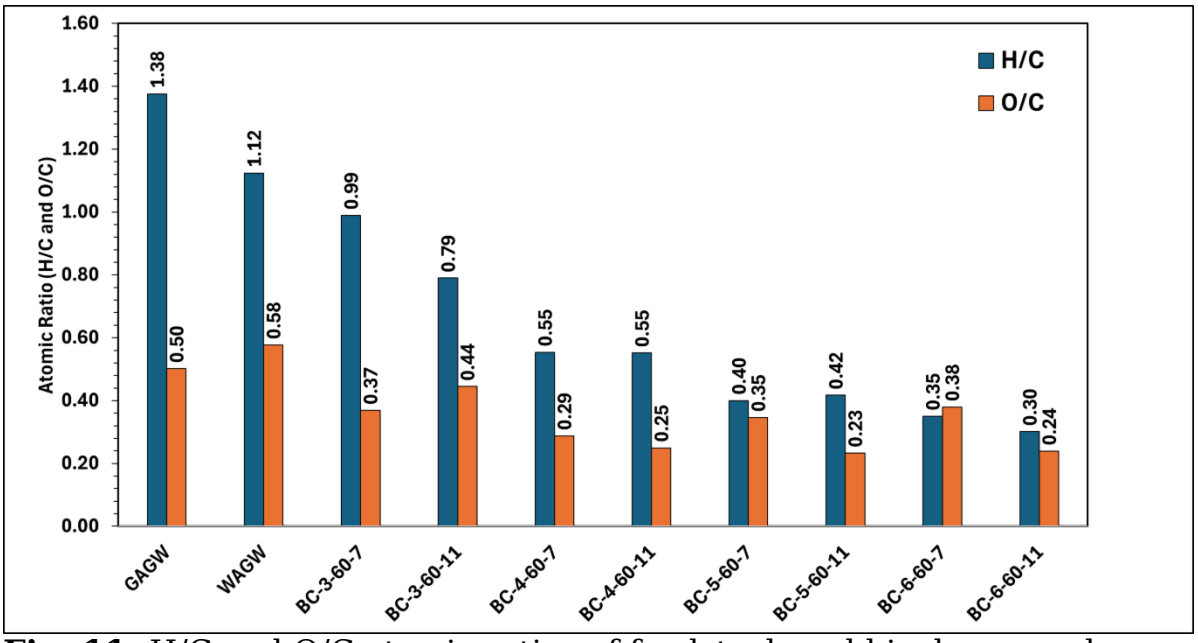

Fig. 11. H/C and O/C atomic ratios of feedstock and biochar samples.

Table 6. Elemental analysis of waste feedstocks and produced biochar samples.

Sample	Ash (%)	N (%)	C (%)	H (%)	S (%)	O (%)	H/C molar ratio	O/C molar ratio
WAGW	6.25	0.54	50.025	4.7178	0	38.47	1.12	0.58
GAGW	13.35	2.32	47.27	5.46	0	31.60	1.38	0.50
BC-3-60-7	9.2	6.42	53.27	4.42	0.49	26.20	0.99	0.37
BC-3-60-11	2.1	0	58.83	3.90	0.32	34.85	0.79	0.44
BC-4-60-7	8	8.37	58.48	2.72	0	22.43	0.55	0.29
BC-4-60-11	2.5	3.49	67.95	3.15	0.28	22.63	0.55	0.25
BC-5-60-7	12	6.09	54.77	1.84	0.04	25.26	0.40	0.35
BC-5-60-11	4	0	71.34	2.5	0	22.16	0.42	0.23
BC-6-60-7	13	5.88	52.84	1.56	0	26.72	0.35	0.38
BC-6-60-11	7	3.82	66.34	1.68	0	21.16	0.30	0.24

Table 7 summarizes the proximate and ultimate properties of biochar produced from various biomass feedstocks under different pyrolysis conditions. The results demonstrate that both feedstock type and pyrolysis temperature strongly influence biochar composition and thermal characteristics. The biochar produced in the present study (BC-6-120-7 and BC-6-120-11) exhibit compositional characteristics consistent with literature-

reported materials produced at comparable temperatures. Their moderate fixed carbon contents, relatively low ash fractions, and elevated carbon percentages indicate successful carbonization under optimized conditions. Moreover, their elemental compositions indicates a balanced combination of structural stability and surface functionality that is characteristic of biochar explored for water treatment and adsorption applications. The comparative analysis in Table 7 highlights the strong coupling between feedstock type, pyrolysis temperature, and biochar composition. High-temperature treatment promotes carbon enrichment, aromaticity, and fixed carbon formation, whereas low-temperature processing preserves volatile compounds and surface functionalities. These trends emphasize the importance of tailoring pyrolysis conditions and feedstock selection to achieve biochar with properties optimized for specific environmental and technological applications. Fig. S3 shows TGA analysis of BC-6-120-7 (a and b) and BC-6-120-11 (c and d).

Table 7. Proximate and ultimate analyses of biochar samples from different biomass feedstocks reported in the literature.

Sample ID	**Feedstock**	**Temperature (°C)**	**MC (%)**	**VM (%)**	**FC (%)**	**Ash (%)**	**C (%)**	**H (%)**	**N (%)**	**S (%)**	**Ref.**
BC700	Date Palm Waste	700	3.48	-	-	20.57	66.70	1.01	0.19	-	[69]
BC900	Date Palm Waste	900	3.06	-	-	21.35	69.38	0.65	0.21	-	[69]
DP-BC (400° C)	Date Palm Fronds	400	4.8	43.2	45.0	7.1	60.9	2.5	1.2	2.2	[70]
RG-BC (400° C)	Rhodes Grass	400	1.8	11.8	56.6	28.8	56.7	2.2	1.9	1.6	[70]
GW	Green waste	-	69.0[a]	68.4[a]	17.4[a]	13.4[a]	44.3[a]	-	1.01[a]	-	[88]
TW250	Woody Chips	250	3.19	81.19	15.51	0.11	52.22	5.18	0.55	-	[62]

TW275	Woody Chips	275	2.90	73.47	23.46	0.17	57.33	4.95	0.37	-	[62]
TW300	Woody Chips	300	2.81	67.58	29.36	0.25	59.03	4.78	0.34	-	[62]
CW325	Carbonized Wood Chips	325	3.29	44.71	51.57	0.43	68.43	4.31	0.35	-	[62]
CW350	Carbonized Wood Chips	350	3.40	43.57	52.56	0.47	69.20	4.28	0.32	-	[62]
CW375	Carbonized Wood Chips	375	4.03	34.13	61.36	0.48	71.39	3.80	0.31	-	[62]
Poplar Biochar	Poplar Wood	600	-	-	-	1-4	88.56-88.89	1.02-1.05	0.64-0.92	-	[71]
ANB-300	Acacia nilotica bark	300	2.67	40.03	57.90	0.93	71.31	3.87	0.35	-	[89]
ANB-600	Acacia nilotica bark	600	1.81	5.84	92.01	2.29	89.80	2.28	0.38	-	[89]
BC-6-120-7	GAGW	600	80.75[b] and 4.2[c]	62.3[c]	23.5[c]	10[c]	51.9	1.1	1.8	0.00	This study
BC-6-120-11	WAGW	600	4[c]	78.9	14.3[c]	2.8[c]-7	61.1	1.4	0.6	0.00	This study

[a]Average values reported in the literature of GW
[b] Moisture content (MC) for fresh green agricultural waste (GAGW)
[c] Based on TGA data of biochar

3.8. Metal Analysis and Safety Assessment of Biomass and Biochar

The metal profiles of both the raw agricultural feedstocks and the resulting biochar samples (BC-6-120-7 and BC-6-120-11) were analyzed to determine their elemental composition and assess their safety for potential environmental applications (Table 8). A crucial finding from this analysis is that both the GAGW and WAGW feedstocks, as well as them pyrolyzed biochar counterparts, were notably free from heavy metals of major public health concern. Essential toxic metals including Arsenic (As), Cadmium (Cd), Chromium (Cr), Lead (Pb), and Mercury (Hg) were all below the analytical detection limit of <0.1 mg/kg. Furthermore, radioactive elements such as Uranium (U) and Thorium (Th) were also absent. This clean elemental profile

is a significant advantage, indicating that the biochar produced from these waste streams pose a low risk of introducing harmful contaminants into the soil or water, supporting their safety profile for a broad range of applications, including agricultural soil amendment [90].

While free from major contaminants, the materials contained several beneficial micronutrients. The GAGW feedstock was particularly rich in Calcium (Ca; 17,629 mg/kg), Potassium (K; 32,503 mg/kg), and Strontium (Sr; 540 mg/kg), with concentrations consistently higher than those in the WAGW feedstock. This trend has also been reported in previous studies [91-93], and is likely attributable to the distinct physiological roles and higher nutrient uptake rates characteristic of green, leafy biomass compared to the more structurally focused woody biomass [94]. Upon pyrolysis, the loss of volatile organic matter led to a significant concentration of these mineral elements in the biochar. Such concentration effects have been previously reported with sludge [95,96]. In this study, this effect was particularly pronounced for Calcium, which increased by approximately 3.6-fold in the GAGW-derived biochar and 6.7-fold in the WAGW-derived biochar. This mineral enrichment enhances the potential value of the biochar as a soil conditioner, capable of returning essential nutrients to the soil but must be cautiously monitored so it does not indue toxicity due to nutrient overload [93] . On the other hand, Tin (Sn), which was present in the feedstocks at 19.4 mg/kg (GAGW) and 23.9 mg/kg (WAGW), showed only a modest increase in concentration in the final biochar (29.9 and 30.9 mg/kg, respectively). This contrasts sharply with the

significant concentration factor observed for elements like Ca and K. The subtle increase in tin concentration may suggest that certain tin compounds could be partially volatilized at the pyrolysis temperature of 600°C [97] which would counteract the concentration effect caused by the loss of biomass. The results of the metal analysis confirm the safety and highlights the potential agronomic value of both biochar, with the GAGW-derived biochar being an especially rich source of key plant-available nutrients.

These findings are also consistent with the expected elemental behavior of the individual feedstocks constituting each composite group. The elevated Ca and K concentrations in GAGW and its derived biochar are characteristic of vegetable and leafy residues, which are physiologically enriched in these macronutrients due to their higher nutrient uptake rates compared to WAGW. The fact that both composite groups behave in a manner fully predictable from their constituent biomass types further confirms that the pooling strategy preserved the essential chemical signatures of each biomass category and did not introduce significant confounding variability into the safety or nutrient assessment.

Table 8: Metal analysis of feedstock and resulting biochar.

Material	**GAGW**	**WAGW**	**BC-6-120-7**	**BC-6-120-11**
Metals (mg/ kg)				
Al	<0.1	<0.1	<0.1	<0.1
As	<0.1	<0.1	<0.1	<0.1
B	<0.1	<0.1	<0.1	<0.1
Ba	10.2	<0.1	28.7	<0.1
Be	<0.1	<0.1	<0.1	<0.1
Ca	17,629	2,354	63,932	15,673
Cd	<0.1	<0.1	<0.1	<0.1

Co	<0.1	<0.1	<0.1	<0.1
Cr	<0.1	<0.1	<0.1	<0.1
Cu	<0.1	<0.1	<0.1	<0.1
Fe	<0.1	<0.1	<0.1	<0.1
Hg	<0.1	<0.1	<0.1	<0.1
K	32,503	7,398	88,780	38,390
Li	<0.1	<0.1	<0.1	<0.1
Mg	<0.1	<0.1	<0.1	<0.1
Mn	25.9	25.3	72.2	69.2
Mo	<0.1	<0.1	<0.1	<0.1
Na	<0.1	<0.1	<0.1	<0.1
Ni	<0.1	<0.1	<0.1	<0.1
P	<0.1	<0.1	<0.1	<0.1
Pb	<0.1	<0.1	<0.1	<0.1
Si	<0.1	<0.1	<0.1	<0.1
Sb	<0.1	<0.1	<0.1	<0.1
Sn	19.4	23.9	29.9	30.9
Sr	540	167	1,635	389
Th	<0.1	<0.1	<0.1	<0.1
Tl	<0.1	<0.1	<0.1	<0.1
U	<0.1	<0.1	<0.1	<0.1
V	<0.1	<0.1	<0.1	<0.1
Zn	<0.1	<0.1	<0.1	<0.1

Note: <0.1 mg/kg indicate that measured values fell below this analytical detection threshold.

The elemental composition of the raw feedstocks (GAGW and WAGW) and their corresponding biochar samples (BC-6-120-7 and BC-6-120-11) was systematically evaluated using ICP-OES and XRF to assess metal content, ash chemistry, and environmental safety (Table 8 and Table 2). The ICP-OES results show that potentially toxic elements such as As, Cd, Cr, Cu, Hg, Ni, Pb, Zn, Sb, Tl, and U were below the detection limit (<0.1 mg kg^{-1}) in both biomass and biochar samples, indicating a low inherent contamination risk and compliance with international biochar safety thresholds, including those defined by the EBC [24].

The elevated Ca and K contents observed by ICP-OES are consistent with the XRF results, which reveal dominant CaO and K_2O phases in the ash fraction, especially for GAGW-derived materials. XRF analysis further highlights compositional differences between GAGW and WAGW ashes. GAGW exhibits higher contents of K_2O, CaO, P_2O_5, SO_3, and Cl, reflecting its nutrient-rich and mineral-dense nature, whereas WAGW shows a significantly higher LOI, indicating a lower inorganic residue. Such differences are critical for environmental applications, as alkaline oxides enhance biochar alkalinity and buffering capacity, which promotes metal immobilization through precipitation, ion exchange, and surface complexation mechanisms [98,99]. From a safety mitigation perspective, the absence of hazardous metals combined with the predominance of benign alkaline and alkaline earth elements confirms that both feedstocks and their derived biochar are environmentally safe for valorization pathways such as soil amendment and pollutant adsorption. Moreover, the transformation of inorganic elements into stable oxide and carbonate phases during pyrolysis reduces metal mobility and bioavailability, further minimizing potential environmental risks [98,100,101].

The relative enrichment factors (RE) was calculated using Eq. 8 as shown in Table 9. The calculated RE values indicate moderate enrichment of alkaline and alkaline earth metals, particularly Ca and K, in WAGW-derived biochar (RE = 2.22-2.84), whereas GAGW-derived biochar exhibited near-unity values (RE = 0.95-1.26). This discrepancy reflects the combined effects

of feedstock composition and mass loss during thermal conversion. Table 9 gives the relative enrichment (RE) factors of selected inorganic nutrients in biochar samples (BC-6-120-7 and BC-6-120-11) derived from GAGW and WAGW, respectively. The results demonstrate a systematic concentration of mineral elements in the biochar relative to their parent feedstocks, primarily because of organic matter volatilization and mass loss during pyrolysis, which leads to the accumulation of thermally stable inorganic constituents in the solid residue [100,102]. Calcium and potassium exhibited the highest enrichment factors, particularly in WAGW-derived biochar (RE = 2.84 and 2.22, respectively), reflecting both the lower initial mineral content of WAGW and the preferential retention of alkaline and alkaline earth elements in the ash fraction during thermal conversion [86,99]. Similar enrichment behavior has been widely reported for lignocellulosic biomass subjected to high-temperature pyrolysis, where Ca and K are predominantly retained in oxide, carbonate, and silicate phases [103,104]. The near-unity values enrichment was observed for manganese and strontium (RE = 1.17-0.99), indicating partial stabilization of these elements within the biochar matrix. This behavior is consistent with previous studies reporting the incorporation of transition and alkaline earth metals into mineral phases during pyrolysis, which enhances their retention and reduces their mobility [101,105]. Generally, the RE analysis confirms that pyrolysis of GAGW and WAGW effectively concentrates essential nutrients while maintaining low levels of potentially toxic elements. These findings are consistent with previous reports on agricultural and

lignocellulosic biomass-derived biochar and emphasize the importance of feedstock selection and process optimization to produce environmentally sustainable biochar [100,103]. In addition, the low levels of potentially toxic elements, supporting the environmentally safe use of the produced biochar for soil amendment and environmental remediation applications [24].

Table 9. Relative Enrichment (RE) Factors of Nutrients in Biochar Derived from green agricultural waste (GAGW) and woody agricultural waste (WAGW).

Element	GAGW (mg/kg)	BC-6-120-7 (mg/kg)	RE (BC-6-120-7, yield-normalized) Yield=34.67 %	WAGW (mg/kg)	BC-6-120-11 (mg/kg)	RE (BC-6-120-11, yield-normalized) Yield = 42.67%
Ca	17,629	63,932	1.26	2,354	15,673	2.84
K	32,503	88,780	0.95	7,398	38,390	2.22
Mn	25.9	72.2	0.97	25.3	69.2	1.17
Sr	540	1,635	1.05	167	389	0.99
Sn	19.4	29.9	0.53	23.9	30.9	0.55
Ba	10.2	28.7	0.97	<0.1*	<0.1*	–

*Elements reported as < 0.1 mg kg^{-1} in feedstocks were excluded from RE calculation.

Relative enrichment factor (RE) was calculated as:

$$RE = \frac{C_{biochar}}{C_{feedstock}} \times \frac{BC\ Yield\ (\%)}{100} \quad (8)$$

where $C_{biochar}$ is the concentration of the element in the biochar samples (BC-6-120-7 and BC-6-120-11), and $C_{feedstock}$is the concentration in the corresponding raw biomass (GAGW and WAGW).

3.9. Economic evaluation of the biochar production process

A preliminary capital cost estimate was developed using the purchase prices of the main laboratory-scale equipment required for biomass drying, grinding, and pyrolysis, as presented in Table 10. Based on the available quotations, the total direct equipment purchase cost is estimated at USD 40,866. This value represents the core process equipment only and excludes installation, instrumentation, utilities, civil works, contingency, and indirect costs.

Table **10**: Capital cost elements of the process.

Equipment	Quantity	Capital cost (USD)	Share of total (%)
Pyrolysis furnace (SH Scientific SH-FU-18.7MHV)	1	34,246	83.8
Drying oven (Binder ED23)	1	5,600	13.7
Grinder / cutting mill (IKA A10)	1	1,020	2.5
Total	3 items	40,866	100.0

The pyrolysis furnace is the dominant capital item, accounting for approximately 83.8% of the total equipment cost, followed by the drying oven at 13.7% and the grinder at 2.5% (Table 10). These results indicate that the

thermal conversion unit is the main economic driver at laboratory scale, and any future scale-up or optimization should primarily focus on reducing reactor-related capital intensity and improving equipment utilization. A simplified techno-economic calculation is performed using the estimated electricity consumption reported in Table 11 together with the direct equipment purchase cost. For transparency, this preliminary analysis assumes an electricity tariff of USD 0.10 per kWh, a project life of 10 years, a discount rate of 8%, and an operating schedule of 250 batches per year. All values should therefore be interpreted as indicative laboratory-scale estimates rather than full commercial production costs.

Table **11**: Pyrolysis energy demands and cost.

Case	**Energy demand (kWh/batch)**	**Electricity cost (USD/batch)**
Low severity pyrolysis	12.5	1.25
High severity pyrolysis	29.3	2.93

Based on these assumptions, the electricity cost is estimated at approximately USD 1.25 per batch under low-severity conditions and USD 2.93 per batch under high-severity conditions. Furthermore, using a capital recovery factor approach, the annualized capital charge for the main equipment is estimated at USD 6,090 per year. When distributed over 250

batches per year, this corresponds to an annualized capital cost of approximately USD 24.36 per batch.

The resulting indicative production costs confirm that energy intensity and biochar yield both strongly affect the unit cost of product. Higher-severity pyrolysis increases electrical consumption and reduces solid yield, leading to a higher cost per kilogram of biochar. The capital cost estimate can be refined further by including the nitrogen supply system required for inert pyrolysis operation. Based on the literature cost range for the gas cylinder, regulator, and fittings, an additional USD 1,500 to 2,000 should be included. This increases the indicative direct equipment purchase cost from USD 40,866 to approximately USD 42,366-42,866. Maintenance cost at laboratory scale is typically estimated at 5-10% of CAPEX per year. On this basis, the annual maintenance requirement is approximately USD 2,118-4,287 per year. Table 12 presents the specific electricity consumption, corresponding electricity cost, and total unit production cost including annualized capital, demonstrating a strong increase in energy demand and cost with higher pyrolysis temperature and highlighting the influence of feedstock type (WAGW vs. GAGW) on process efficiency

Table **12**: Techno-economic assessment of pyrolysis energy demand and unit biochar production cost under varying feedstock types and operating temperatures (300 and 600**°C)**.

Case	Specific electricity demand (kWh/kg biochar)	Electricity cost (USD/kg biochar)	Electricity + annualized capital (USD/kg biochar)
WAGW (300 °C)	18.0	1.80	35.98
GAGW (300 °C)	21.0	2.10	42.70
WAGW (600 °C)	69.0	6.90	63.99
GAGW (600 °C)	84.0	8.40	78.67

For market benchmarking, biochar prices are commonly reported in the range of about USD 300 to over USD 1,300 per ton, depending on product quality, certification status, and end use. This market range is substantially lower than the indicative laboratory-scale production costs estimated in this study, which is expected because bench-scale systems suffer from low throughput, high specific energy demand, and limited process integration. Consequently, the present results should be interpreted primarily as proof-

of-concept techno-economic indicators rather than commercial selling-price estimates.

Using the updated capital cost range, annual maintenance estimate, and electricity consumption derived from the experimental process, the indicative biochar production cost is calculated for each operating case. The calculation combines electricity cost with annualized capital and maintenance charges distributed across 250 batches per year (Fig.12).

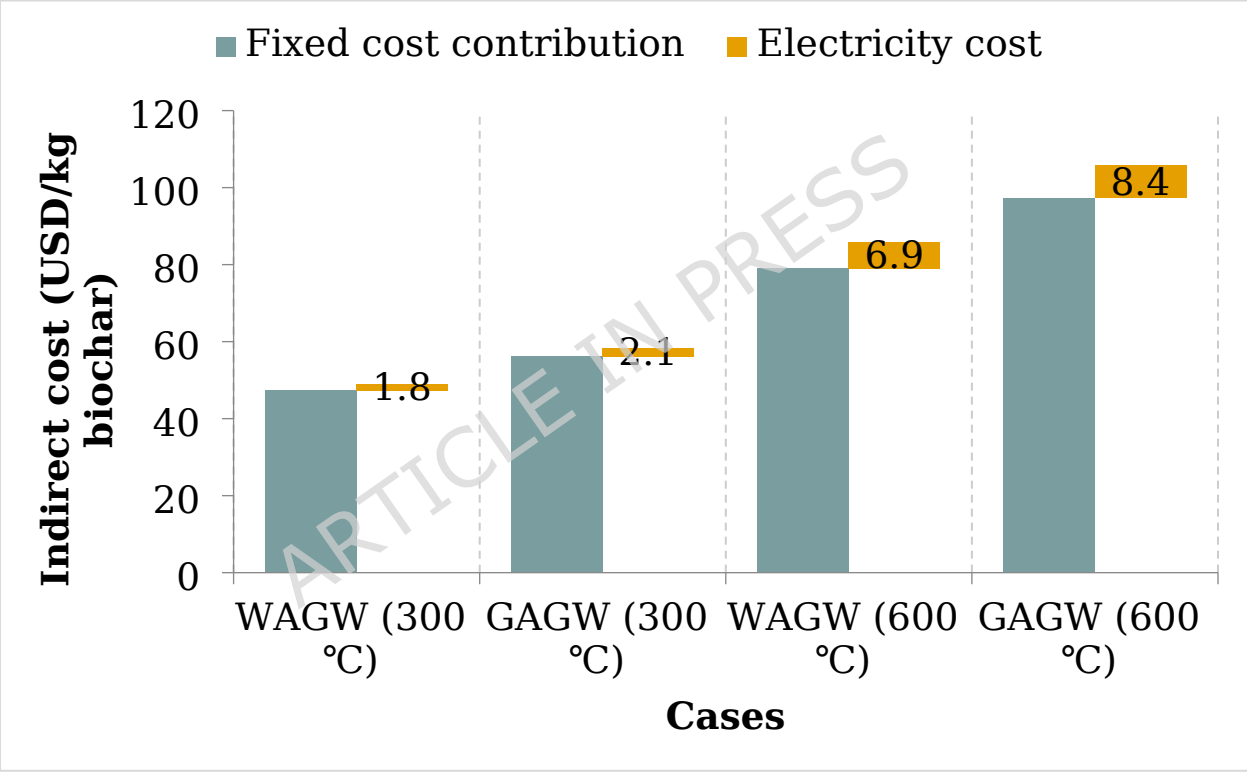

Fig. 12: Cost elements contributions by cases.

As illustrated in Fig. 13, the estimated production cost ranges from approximately USD 49.1 to 131.6 per kg of biochar, depending on feedstock type and pyrolysis severity. The lowest cost is obtained for WAGW at 300 ℃, while the highest cost is obtained for GAGW at 600 ℃. This confirms that the

current laboratory configuration is not economically competitive with typical market prices and should therefore be viewed primarily as a proof-of-concept research system rather than a commercially optimized production process.

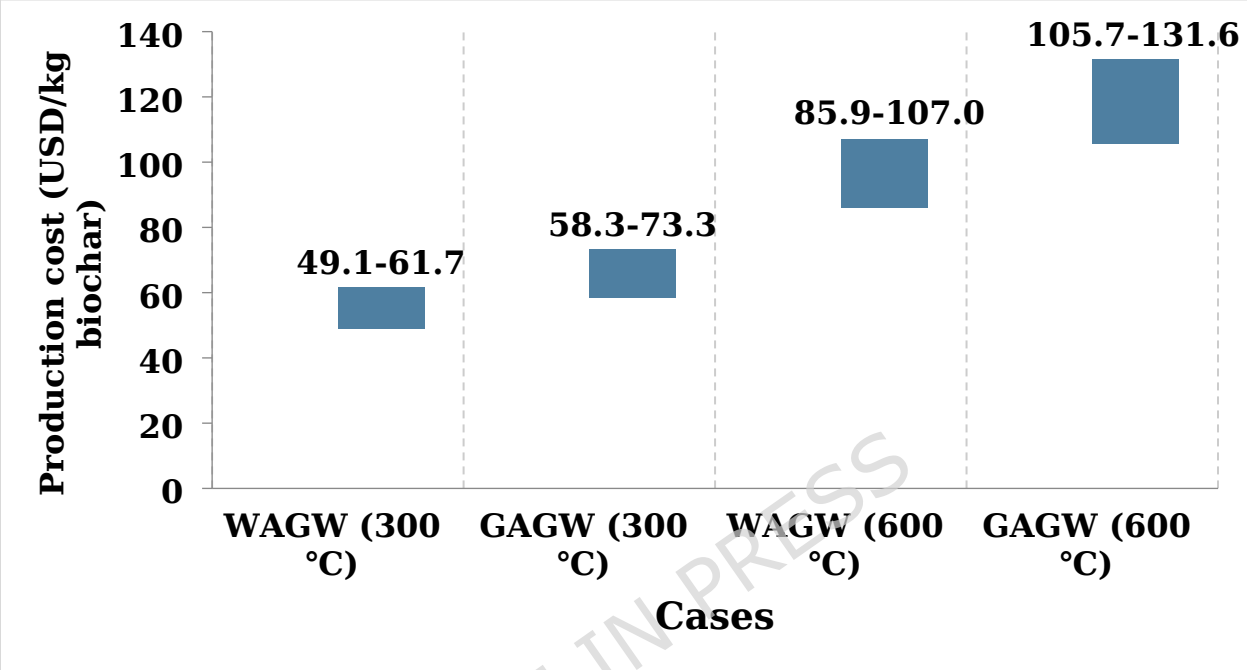

Fig. 13: Estimated biochar production cost range for different feedstocks and pyrolysis conditions.

4. Conclusions

This study investigated the production and multi-scale characterization of biochar production from two mixed AGW biomass collected from local farms in Qatar. Each feedstock underwent comprehensive characterization to assess its suitability for biochar production. The pyrolysis process was conducted at temperatures (300-600 °C) and durations (20-120 min). Results showed that biochar yield generally decreased with increasing temperature and residence time, indicating enhanced devolatilization and carbonization

at higher thermal conditions. Among the tested feedstocks, WAGW from HSF exhibited the highest biochar yield (71.28%) when pyrolyzed at 300 °C for 20 min. This sample also had a relatively low ash content (2.1- 6.25%), making it favorable for applications such as soil amendment and carbon sequestration. Furthermore, BET analysis revealed that WAGW biochar had the highest specific surface area (684 m^2/g), a property associated in the literature with potential utility in environmental remediation and soil amendment applications, which represents a promising direction for future experimental investigation. These results demonstrate that woody agricultural residues from HSF are particularly promising for sustainable biochar production in Qatar. The study contributes to identifying optimal local biomass and pyrolysis conditions for producing high-quality biochar for agricultural and environmental applications. The XRF patterns indicate that GAGW is better suited for nutrient-rich, ash-active biochar products, while WAGW is ideal for high-carbon, adsorption-oriented, or carbon-sequestration biochar. The RE is a critical parameter for evaluating the functional performance and environmental safety of biochar intended for water treatment systems. In the Qatari context, WAGW-derived biochar is particularly suited for adsorption-based treatment of brackish and produced water, while GAGW-derived biochar offers potential for soil conditioning and nutrient retention in arid desert farming systems. This study is scoped as a systematic evaluation of biochar production, characterization, and safety.

Application-specific performance validation under the local arid conditions is identified as a critical next step and is strongly recommended.

Acknowledgements

The authors sincerely acknowledge the Qatar Environment and Energy Research Institute and Hamad Bin Khalifa University for their invaluable support. They also thank HBKU Core Labs for conducting the analytical analysis. Furthermore, the authors appreciate the local farms in Qatar for their assistance in biomass collection. The authors gratefully acknowledge Dr. Jamileh Fouladi for her valuable contribution in conducting the economic evaluation of the biochar production process. Open access funding provided by the Qatar National Library.

Declaration of Interest Statement

The authors declare that they have no known competing financial interests or personal relationships that could have influenced the work reported in this study.

Author contributions

Rashad Al-Gaashani: The first and corresponding author, Methodology, Data curation, Writing – original draft, Validation, Investigation, Conceptualization, Writing – review & editing. **Omar Shahid:** Methodology, Formal analysis, Writing – review & editing. **Ojima Z. Wada**: Formal analysis, Writing – review & editing. **Simjo Simson**: Formal analysis. **Tricia A. Gomez:** Formal analysis**. Mujaheed Pasha:** Formal analysis. **Omar El Hassan:** Formal analysis. **Abdulaziz Suwailem:** Formal analysis. **Kashif**

Rasool: Writing – review & editing, project administration. **Gordon McKay:** Writing – review & editing, Supervision. **Tareq Al-Ansari:** Writing – review & editing, Supervision. **Khaled A. Mahmoud:** Writing – review & editing, Project administration, Supervision.

Data availability

The datasets used and/or analyzed during the current study available from the corresponding author on reasonable request.

Funding

No funding.

References

1 Khan, M. N., Sial, T. A., Ali, A. & Wahid, F. in *Frontier Studies in Soil Science* 79-108 (Springer, 2024).
2 Maji, S., Dwivedi, D. H., Singh, N., Kishor, S. & Gond, M. Agricultural waste: Its impact on environment and management approaches. *Emerging eco-friendly green technologies for wastewater treatment*, 329-351 (2020).
3 Dhamodharan, K., Konduru, T., Kannan, M. & Malyan, S. K. in *Emerging trends to approaching zero waste* 243-264 (Elsevier, 2022).
4 Maraveas, C. Production of sustainable and biodegradable polymers from agricultural waste. *Polymers* **12**, 1127, doi:10.3390/polym12051127 (2020).
5 Zafar, S. in *The palgrave handbook of sustainability: case studies and practical solutions* 159-181 (Springer, 2018).
6 Mariyam, S., Cochrane, L., Zuhara, S. & McKay, G. Waste management in Qatar: A systematic literature review and recommendations for system strengthening. *Sustainability* **14**, 8991, doi:ARTN 899110.3390/su14158991 (2022).
7 Chen, W.-H. *et al.* Current status of biohydrogen production from lignocellulosic biomass, technical challenges and commercial potential through pyrolysis process. *Energy* **226**, 120433 (2021).
8 Calabrò, P. S. Greenhouse gases emission from municipal waste management: The role of separate collection. *Waste management* **29**, 2178-2187, doi:https://doi.org/10.1016/j.wasman.2009.02.011 (2009).

9 Wihersaari, M. Evaluation of greenhouse gas emission risks from storage of wood residue. *Biomass and Bioenergy* **28**, 444-453, doi:https://doi.org/10.1016/j.biombioe.2004.11.011 (2005).
10 Zhang, X. *et al.* A review of converting woody biomass waste into useful and eco-friendly road materials. *Transportation Safety and Environment* **4**, tdab031 (2022).
11 Lehmann, J. & Joseph, S. *Biochar for environmental management: science and technology*. (Routledge, 2012).
12 Sohi, S., Lopez-Capel, E., Krull, E. & Bol, R. Biochar, climate change and soil: A review to guide future research. *CSIRO land and water science report* **5**, 17-31 (2009).
13 Azim, R. *et al.* Exploring the potential of straw and biochar application on soil quality indicators and crop yield in semi-arid regions. *Journal of Soil Science and Plant Nutrition* **24**, 1907-1923, doi:10.1007/s42729-024-01668-2 (2024).
14 Xiao, Q. *et al.* Soil amendment with biochar increases maize yields in a semi-arid region by improving soil quality and root growth. *Crop and Pasture Science* **67**, 495-507, doi:10.1071/Cp15351 (2016).
15 Abdelhak, M. in *Natural resources conservation and advances for sustainability* 73-90 (Elsevier, 2022).
16 Diatta, A. A., Fike, J. H., Battaglia, M. L., Galbraith, J. M. & Baig, M. B. Effects of biochar on soil fertility and crop productivity in arid regions: a review. *Arabian Journal of Geosciences* **13**, 1-17, doi:ARTN 595
10.1007/s12517-020-05586-2 (2020).
17 Obar, F., Alherbawi, M., Mckay, G. & Al-Ansari, T. Optimizing the utilization of biochar from waste: an energy–water–food nexus assessment approach considering water treatment and soil application scenarios. *Frontiers in Environmental Science* **11**, 1238810, doi:ARTN 1238810
10.3389/fenvs.2023.1238810 (2023).
18 Pradhan, S., Mackey, H. R., Al-Ansari, T. & McKay, G. Biochar: a sustainable approach for water stress and plant growth. *International Journal of Global Warming* **25**, 425-439, doi:10.1504/Ijgw.2021.119010 (2021).
19 Al-Rumaihi, A. *et al.* Assessing plastic and biomass-based biochar's potential for carbon sequestration: an energy-water-environment approach. *Frontiers in Sustainability* **4**, 1200094, doi:ARTN 1200094
10.3389/frsus.2023.1200094 (2023).
20 Parthasarathy, P., Alherbawi, M., Pradhan, S., Al-Ansari, T. & McKay, G. Estimation of Poultry Litter and its Biochar Production Potential through Pyrolysis in Qatar. *Chemical Engineering Transactions* **109**, 229-234 (2024).
21 Elkhalifa, S. *et al.* in *Computer Aided Chemical Engineering* Vol. 46 901-906 (Elsevier, 2019).

22 Pradhan, S. *et al.* A comprehensive decision-making approach for the application of biochar in agriculture to enhance water security: A GIS-AHP based approach. *Environmental Technology & Innovation* **36**, 103801, doi:ARTN 103801
10.1016/j.eti.2024.103801 (2024).
23 Ghiat, I. *et al.* Biochar: a sustainable approach of green waste management in agricultural practices under controlled microclimate. *Chemical Engineering Transactions* **92**, 331-336 (2022).
24 Schmidt, H. P. *et al.* European biochar certificate-guidelines for a sustainable production of biochar. (2016).
25 Meyer, S. *et al.* Biochar standardization and legislation harmonization. *Journal of Environmental Engineering and Landscape Management* **25**, 175-191 (2017).
26 Major, J. A guide to conducting biochar trials. *International Biochar Initiaive*, 4-27 (2009).
27 Pourhashem, G., Hung, S. Y., Medlock, K. B. & Masiello, C. A. Policy support for biochar: Review and recommendations. *GCB Bioenergy* **11**, 364-380 (2019).
28 Nepal, J., Ahmad, W., Munsif, F., Khan, A. & Zou, Z. Advances and prospects of biochar in improving soil fertility, biochemical quality, and environmental applications. *Frontiers in Environmental Science* **11**, 1114752 (2023).
29 Enaime, G., Baçaoui, A., Yaacoubi, A. & Lübken, M. Biochar for wastewater treatment—conversion technologies and applications. *Applied Sciences* **10**, 3492 (2020).
30 Inyang, M. & Dickenson, E. The potential role of biochar in the removal of organic and microbial contaminants from potable and reuse water: A review. *Chemosphere* **134**, 232-240 (2015).
31 He, M. *et al.* Waste-derived biochar for water pollution control and sustainable development. *Nature Reviews Earth & Environment* **3**, 444-460 (2022).
32 Ippolito, J. A. *et al.* Feedstock choice, pyrolysis temperature and type influence biochar characteristics: a comprehensive meta-data analysis review. *Biochar* **2**, 421-438 (2020).
33 Tomczyk, A., Sokołowska, Z. & Boguta, P. Biochar physicochemical properties: pyrolysis temperature and feedstock kind effects. *Reviews in Environmental Science and Bio/Technology* **19**, 191-215 (2020).
34 Wystalska, K. & Kwarciak-Kozłowska, A. The effect of biodegradable waste pyrolysis temperatures on selected biochar properties. *Materials* **14**, 1644 (2021).
35 Zhao, B. *et al.* Effect of pyrolysis temperature, heating rate, and residence time on rapeseed stem derived biochar. *Journal of Cleaner Production* **174**, 977-987 (2018).
36 Han, L. *et al.* Impact of biochar amendment on soil aggregation varied with incubation duration and biochar pyrolysis temperature. *Biochar* **3**, 339-347 (2021).

37 Shaaban, A. *et al.* Influence of heating temperature and holding time on biochars derived from rubber wood sawdust via slow pyrolysis. *Journal of Analytical and Applied Pyrolysis* **107**, 31-39 (2014).
38 *Standard Test Method for Chemical Analysis of Wood Charcoal*. (ASTM International, 2021).
39 Jabeen, S. *et al.* Analytical procedure for proximate analysis of algal biomass: Case study for Spirulina platensis and Chlorella vulgaris. *Energy & Fuels* **34**, 474-482 (2019).
40 Bhattacharjee, N. & Biswas, A. B. Pyrolysis of Alternanthera philoxeroides (alligator weed): Effect of pyrolysis parameter on product yield and characterization of liquid product and bio char. *Journal of the Energy Institute* **91**, 605-618 (2018).
41 Akça, M. O., Ok, S. S., Deniz, K., Mohammedelnour, A. & Kibar, M. Spectroscopic characterisation and elemental composition of biochars obtained from different agricultural wastes. *Journal of Agricultural Sciences* **27**, 426-435 (2021).
42 Mikajlo, I. *et al.* Composted biochar versus compost with biochar: effects on soil properties and plant growth. *Biochar* **6**, 85 (2024).
43 Domingues, R. R. *et al.* Properties of biochar derived from wood and high-nutrient biomasses with the aim of agronomic and environmental benefits. *PloS one* **12**, e0176884 (2017).
44 Sadasivam, B. Y. & Reddy, K. R. Engineering properties of waste wood-derived biochars and biochar-amended soils. *International Journal of Geotechnical Engineering* **9**, 521-535 (2015).
45 Chojnacka, K., Gil, F., Skrzypczak, D. & Izydorczyk, G. in *Sustainable Fertilizers: Utilizing Biomass Ashes and Biochars: Transforming Waste into Agricultural Products* 9-19 (Springer, 2025).
46 Butphu, S., Rasche, F., Cadisch, G. & Kaewpradit, W. Eucalyptus biochar application enhances Ca uptake of upland rice, soil available P, exchangeable K, yield, and N use efficiency of sugarcane in a crop rotation system. *Journal of Plant Nutrition and Soil Science* **183**, 58-68 (2020).
47 Godiya, C. B. & Leiviskä, T. Wood-derived adsorbents for the removal of pharmaceutical contamination from wastewater: a review. *Environmental Chemistry Letters*, 1-31 (2025).
48 Zhao, L., Cao, X., Zheng, W., Wang, Q. & Yang, F. Endogenous minerals have influences on surface electrochemistry and ion exchange properties of biochar. *Chemosphere* **136**, 133-139 (2015).
49 Novak, J. M. *et al.* Characterization of designer biochar produced at different temperatures and their effects on a loamy sand. *Annals of environmental science* (2009).
50 Gezahegn, S. *Wood and Bamboo Biochars and Their Application in Soils and Biocomposites*. (University of Toronto (Canada), 2020).
51 Singh, B., Dolk, M. M., Shen, Q. & Camps-Arbestain, M. Biochar pH, electrical conductivity and liming potential. *Biochar: A guide to analytical methods* **23** (2017).

52 Li, X. *et al.* Functional groups determine biochar properties (pH and EC) as studied by two-dimensional 13C NMR correlation spectroscopy. *PLoS One* **8**, e65949 (2013).
53 Kritikaki, A., Karmali, V., Vathi, D., Bartzas, G. & Komnitsas, K. Advanced Characterization of Biochars Produced from Three Different Organic-based Feedstocks and their Potential Applications. *Circular Economy and Sustainability*, 1-24 (2025).
54 Kan, T., Strezov, V. & Evans, T. J. Lignocellulosic biomass pyrolysis: A review of product properties and effects of pyrolysis parameters. *Renewable and sustainable energy reviews* **57**, 1126-1140 (2016).
55 Ma, Z., Chen, D., Gu, J., Bao, B. & Zhang, Q. Determination of pyrolysis characteristics and kinetics of palm kernel shell using TGA–FTIR and model-free integral methods. *Energy Conversion and Management* **89**, 251-259 (2015).
56 Elder, J. P. Proximate analysis by automated thermogravimetry. *Fuel* **62**, 580-584 (1983).
57 Danias, P. & Liodakis, S. Characterization of refuse derived fuel using thermogravimetric analysis and chemometric techniques. *Journal of Analytical Chemistry* **73**, 351-357 (2018).
58 Park, S. *et al.* Thermogravimetric analysis-based proximate analysis of agro-byproducts and prediction of calorific value. *Energy Reports* **8**, 12038-12044 (2022).
59 Antal, M. J. & Grønli, M. The art, science, and technology of charcoal production. *Industrial & engineering chemistry research* **42**, 1619-1640 (2003).
60 Al-Rumaihi, A., Shahbaz, M., Mckay, G., Mackey, H. & Al-Ansari, T. A review of pyrolysis technologies and feedstock: A blending approach for plastic and biomass towards optimum biochar yield. *Renewable and Sustainable Energy Reviews* **167**, 112715 (2022).
61 Parvari, E., Mahajan, D. & Hewitt, E. L. A Review of Biomass Pyrolysis for Production of Fuels: Chemistry, Processing, and Techno-Economic Analysis. *Biomass* **5**, 54 (2025).
62 Park, S.-W., Jang, C.-H., Baek, K.-R. & Yang, J.-K. Torrefaction and low-temperature carbonization of woody biomass: Evaluation of fuel characteristics of the products. *Energy* **45**, 676-685 (2012).
63 Yang, H., Yan, R., Chen, H., Lee, D. H. & Zheng, C. Characteristics of hemicellulose, cellulose and lignin pyrolysis. *Fuel* **86**, 1781-1788 (2007).
64 Nelson, N., Darkwa, J. & Calautit, J. Prospects of bioenergy production for sustainable rural development in Ghana. *Journal of Sustainable Bioenergy Systems* **11**, 227-259 (2021).
65 Sansaniwal, S., Rosen, M. & Tyagi, S. Global challenges in the sustainable development of biomass gasification: An overview. *Renewable and Sustainable Energy Reviews* **80**, 23-43 (2017).

66 Yorgun, S. & Yıldız, D. Slow pyrolysis of paulownia wood: Effects of pyrolysis parameters on product yields and bio-oil characterization. *Journal of analytical and applied pyrolysis* **114**, 68-78 (2015).
67 Cloke, M., Lester, E. & Leney, M. Effect of volatile retention on the products from low temperature pyrolysis in a fixed bed batch reactor. *Fuel* **78**, 1719-1728 (1999).
68 Apaydın Varol, E. & Mutlu, Ü. TGA-FTIR analysis of biomass samples based on the thermal decomposition behavior of hemicellulose, cellulose, and lignin. *Energies* **16**, 3674 (2023).
69 Poulose, A. M. *et al.* Date palm biochar-polymer composites: An investigation of electrical, mechanical, thermal and rheological characteristics. *Science of the total environment* **619**, 311-318 (2018).
70 Jouiad, M., Al-Nofeli, N., Khalifa, N., Benyettou, F. & Yousef, L. F. Characteristics of slow pyrolysis biochars produced from rhodes grass and fronds of edible date palm. *Journal of analytical and applied pyrolysis* **111**, 183-190 (2015).
71 Chen, D. *et al.* Pyrolysis polygeneration of poplar wood: Effect of heating rate and pyrolysis temperature. *Bioresource Technology* **218**, 780-788 (2016).
72 Kouchachvili, L., Gagnon-Caya, G. & Djebbar, R. Wood-derived biochar as a matrix for cost-effective and high-performing composite thermal energy storage materials. *Journal of Porous Materials* **32**, 55-66 (2025).
73 Joseph, S. *Biochar for environmental management: science, technology and implementation*. (Routledge, 2015).
74 Mackay, D. & Roberts, P. The influence of pyrolysis conditions on yield and microporosity of lignocellulosic chars. *Carbon* **20**, 95-104 (1982).
75 Chen, W. *et al.* Characteristics of wood-derived biochars produced at different temperatures before and after deashing: their different potential advantages in environmental applications. *Science of the Total Environment* **651**, 2762-2771 (2019).
76 Miyata, T., Endo, A., Ohmori, T., Akiya, T. & Nakaiwa, M. Evaluation of pore size distribution in boundary region of micropore and mesopore using gas adsorption method. *Journal of colloid and interface science* **262**, 116-125 (2003).
77 Ou, M.-J. Y., De Paolis, A. & Cardoso, L. Mathematical Quantification of the Impact of Microstructure on the Various Effective Properties of Bones. (2019).
78 Domokos-Szabolcsy, É. *et al.* Green biomass-based protein for sustainable feed and food supply: an overview of current and future prospective. *Life* **13**, 307, doi:https://doi.org/10.3390/life13020307 (2023).
79 Wijeyekoon, S. L. & Vaidya, A. A. Woody biomass as a potential feedstock for fermentative gaseous biofuel production. *World Journal of Microbiology and Biotechnology* **37**, 134, doi:https://doi.org/10.1007/s11274-021-03102-6 (2021).

80 Musa, A. M., Ishak, C. F., Karam, D. S. & Md Jaafar, N. Effects of fruit and vegetable wastes and biodegradable municipal wastes co-mixed composts on nitrogen dynamics in an Oxisol. *Agronomy* **10**, 1609, doi:https://doi.org/10.3390/agronomy10101609 (2020).
81 Muley, P. D., Henkel, C., Abdollahi, K. K., Marculescu, C. & Boldor, D. A critical comparison of pyrolysis of cellulose, lignin, and pine sawdust using an induction heating reactor. *Energy conversion and management* **117**, 273-280, doi:https://doi.org/10.1016/j.enconman.2016.03.041 (2016).
82 Li, C.-Z. & Tan, L. L. Formation of NOx and SOx precursors during the pyrolysis of coal and biomass. Part III. Further discussion on the formation of HCN and NH3 during pyrolysis. *Fuel* **79**, 1899-1906, doi:https://doi.org/10.1016/S0016-2361(00)00008-9 (2000).
83 Li, S. Reviewing air pollutants generated during the pyrolysis of solid waste for biofuel and biochar production: toward cleaner production practices. *Sustainability* **16**, 1169 (2024).
84 Wei, L. *et al.* The ratio of H/C is a useful parameter to predict adsorption of the herbicide metolachlor to biochars. *Environmental research* **184**, 109324, doi:ARTN 109324
10.1016/j.envres.2020.109324 (2020).
85 Keiluweit, M., Nico, P. S., Johnson, M. G. & Kleber, M. Dynamic molecular structure of plant biomass-derived black carbon (biochar). *Environmental science & technology* **44**, 1247-1253, doi:https://doi.org/10.1021/es9031419 (2010).
86 Enders, A., Hanley, K., Whitman, T., Joseph, S. & Lehmann, J. Characterization of biochars to evaluate recalcitrance and agronomic performance. *Bioresource technology* **114**, 644-653, doi:https://doi.org/10.1016/j.biortech.2012.03.022 (2012).
87 Spokas, K. A. Review of the stability of biochar in soils: predictability of O: C molar ratios. *Carbon management* **1**, 289-303, doi:https://www.tandfonline.com/action/showCitFormats?doi=10.4155/cmt.10.32 (2010).
88 Liu, X., Xie, Y. & Sheng, H. Green waste characteristics and sustainable recycling options. *Resources, Environment and Sustainability* **11**, 100098, doi:https://doi.org/10.1016/j.resenv.2022.100098 (2023).
89 Murtaza, G. *et al.* Liming potential and characteristics of biochar produced from woody and non-woody biomass at different pyrolysis temperatures. *Scientific Reports* **14**, 11469 (2024).
90 Srinivasan, P. *et al.* A feasibility study of agricultural and sewage biomass as biochar, bioenergy and biocomposite feedstock: production, characterization and potential applications. *Science of the total environment* **512**, 495-505, doi:10.1016/j.scitotenv.2015.01.068 (2015).
91 Singh, B., Camps-Arbestain, M. & Lehmann, J. *Biochar: a guide to analytical methods*. (Csiro Publishing, 2017).

92 Zhao, L., Cao, X., Wang, Q., Yang, F. & Xu, S. Mineral constituents profile of biochar derived from diversified waste biomasses: implications for agricultural applications. *Journal of Environmental Quality* **42**, 545-552, doi:10.2134/jeq2012.0232 (2013).
93 Enders, A., Sohi, S., Lehmann, J. & Singh, B. Total elemental analysis of metals and nutrients in biochar. *Biochar: A Guide to Analytical Methods* **1** (2017).
94 Elbersen, W. *et al.* in *Modeling and Optimization of Biomass Supply Chains* 55-78 (Elsevier, 2017).
95 Jin, J. *et al.* Influence of pyrolysis temperature on properties and environmental safety of heavy metals in biochars derived from municipal sewage sludge. *Journal of hazardous materials* **320**, 417-426, doi:10.1016/j.jhazmat.2016.08.050 (2016).
96 Wang, X., Li, C., Li, Z., Yu, G. & Wang, Y. Effect of pyrolysis temperature on characteristics, chemical speciation and risk evaluation of heavy metals in biochar derived from textile dyeing sludge. *Ecotoxicology and Environmental Safety* **168**, 45-52, doi:10.1016/j.ecoenv.2018.10.022 (2019).
97 Han, S. *et al.* Mitigating heavy metal volatilization during thermal treatment of MSWI fly ash by using iron (III) sulfate as a chlorine depleting agent. *Journal of Hazardous Materials* **465**, 133185 (2024).
98 Beesley, L., Moreno-Jiménez, E. & Gomez-Eyles, J. L. Effects of biochar and greenwaste compost amendments on mobility, bioavailability and toxicity of inorganic and organic contaminants in a multi-element polluted soil. *Environmental pollution* **158**, 2282-2287 (2010).
99 Novak, J. M. *et al.* Impact of biochar amendment on fertility of a southeastern coastal plain soil. *Soil science* **174**, 105-112 (2009).
100 Hossain, M. K., Strezov, V., Chan, K. Y., Ziolkowski, A. & Nelson, P. F. Influence of pyrolysis temperature on production and nutrient properties of wastewater sludge biochar. *Journal of environmental management* **92**, 223-228, doi:https://doi.org/10.1016/j.jenvman.2010.09.008 (2011).
101 Ahmad, M. *et al.* Biochar as a sorbent for contaminant management in soil and water: a review. *Chemosphere* **99**, 19-33, doi:https://doi.org/10.1016/j.chemosphere.2013.10.071 (2014).
102 Cantrell, K. B., Hunt, P. G., Uchimiya, M., Novak, J. M. & Ro, K. S. Impact of pyrolysis temperature and manure source on physicochemical characteristics of biochar. *Bioresource technology* **107**, 419-428, doi:https://doi.org/10.1016/j.biortech.2011.11.084 (2012).
103 Nan, H. *et al.* Pyrolysis temperature-dependent carbon retention and stability of biochar with participation of calcium: Implications to carbon sequestration. *Environmental Pollution* **287**, 117566, doi:https://doi.org/10.1016/j.envpol.2021.117566 (2021).
104 Thyrel, M., Backman, R., Boström, D., Skyllberg, U. & Lestander, T. A. Phase transitions involving Ca–The most abundant ash forming

element–In thermal treatment of lignocellulosic biomass. *Fuel* **285**, 119054, doi:https://doi.org/10.1016/j.fuel.2020.119054 (2021).
105 Yu, Q. *et al.* Impact of blending on hydrolysis and ethanol fermentation of garden wastes. *Journal of Cleaner Production* **190**, 36-43, doi:https://doi.org/10.1016/j.jclepro.2018.04.164 (2018).